

Virus like particles: fundamental concepts, biological interactions, and clinical applications

Candace Benjamin*, Olivia Brohlin*, Arezoo Shahrivarkevishahi and Jeremiah J. Gassensmith

Department of Chemistry and Biochemistry, University of Texas at Dallas, Richardson, Texas, United States

11.1 Introduction

Nanotechnology has offered hopes for the delivery of new technologies in medicine and drug delivery, yet a growing number of voices have begun to express skepticism¹ that these long sought advances may have been over promised.² Specifically, issues with targeting and delivering payloads have been called out as being difficult obstacles that still need to be overcome.³ The reasons for these shortcomings are multiple and linked to issues with biocompatibility,⁴ bioaccumulation,⁵ and pharmacokinetics,^{6,7} all of which can be addressed through clever materials chemistry and bioengineering. The present and persistent issue in nanotech, we must remember, is the “tech” and not the “nano.” Nature has very effectively employed nanoscale delivery vehicles for highly selective and targeted gene delivery in the form of viruses. Indeed, their efficacy in delivering sickness to people has created some skepticism to their use, but recent efforts to chemically and biologically engineer “virus-like particles” (VLPs) that take structural cues from these natural nanoparticles have begun to yield important new medicines. For instance, one oncolytic viral nanoparticle^{8,9} has made it to the clinic^{10–12} and is saving lives,^{10,13–15} but many more are in the FDA’s approval pipeline and even more are active targets of research for delivery, imaging, stimulation, and biosensing applications.

Viral capsids are extremely useful for these applications as they are easy to produce and straightforward to employ. This is simply owing to the biological nature of the VLP, which imbues five major aspects that define the capsids’

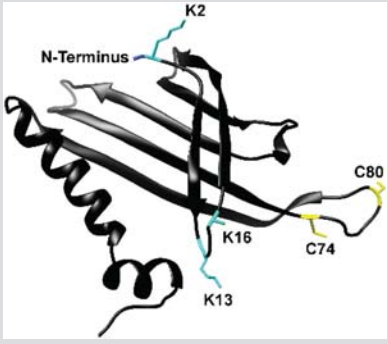
value in these fields: (1) ease of production, (2) ability to self-assemble, (3) facile modification, (4) biocompatibility, and (5) immunogenicity. To date, more than 30 different VLPs have been generated⁷¹ through the removal and replacement of the natural viral genome with a modified set of genetic material. These “stripped down” versions spontaneously assemble in noninfectious^{72,73} analogs of their viral parents that lack an ability to self-proliferate while preserving many of the other native viral traits. VLPs, typically 15–400 nm,⁷⁴ can be replicated and purified from many heterologous expression systems such as bacteria, plants, and yeast⁷⁵ to produce ready-to-use nanoparticles for further modification. These methods of replication allow for the scalable production of uniform VLPs with a narrow size distribution, which is crucial for medical applications. These characteristics permit more precise loading of cargos inside of the carrier and regularly spaced functional handles, most commonly lysines, tyrosines, glutamates, aspartates, and cysteines for the development of a multifunctional nanocarrier (Table 11.1). Multiple conjugates can also be attached as a cargo to VLPs, thanks to the multivalency of these subunits that make up the virus including bimodal imaging agents,⁷⁶ targeted biosensors,^{77,78} and shielded drug carriers.^{79,80} Biodistribution studies have been performed using a few of the icosahedral VLPs, which show the particles mostly accumulate in the liver and spleen^{81,82} and are usually cleared within 24 h.⁸³ These carriers can be further modified to help determine their in vivo fate by installing moieties designed to alter the surface charge of the particle^{84,85} or stealth capability^{86–88}

* These authors contributed equally to this manuscript.

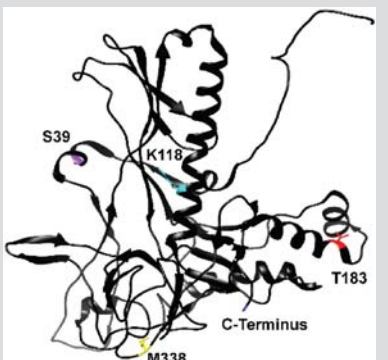
TABLE 11.1 Examples of bioconjugation reactions on popular virus-like particles.

	Residue	Chemical reaction	Incorporated material
MS2			
	Y85	Diazotization	Diazonium salt, ¹⁶ FAM-SE, ¹⁷ [¹⁸ F]-benzaldehyde, ¹⁸ Gd(III) complex ¹⁹
		Potassium ferricyanide-mediated oxidative coupling	Gold NPs ²⁰
	T19pAF	NaO ₄ -mediated oxidative coupling	AF 488, ²¹ DNA, ²¹ DNA aptamers, ²² fibrin, ²³ peptides, ²⁴ PEG, ²⁵ porphyrin ²⁶
		Photolysis/coupling with aniline groups	DNA ²⁷
	N87C	Thiol-maleimide	AF 488, ²² AF 680, ²³ DOTA, ²⁵ AF 350, ²⁶ Oregon Green 488, ²⁶ Gd(III) complex, ²⁸ Taxol ²⁹
K106, K113, N-terminus	Isothiocyanate coupling	PEG ¹⁷ TREN-bis-HOPO-TAM ligand ¹⁹	
TMV			
	Y139	Diazotization and oximation	Diazonium salts and alkoxyamines ³⁰
		Iodogen method	Na ¹²⁵ I ³¹
		Diazotization/CuAAC	Gd(DOTA), ^{32,33} Tn antigen, ³⁴ pyrene PEG, ³⁵ RGD peptide, ³⁶ β-cyclodextrin, ³⁷ oligoaniline ³⁸
	E97, E106	Amide formation/CuAAC	PEG ³²
		Amide formation	Amines ³⁰
	S123C	Maleimide coupling/CuAAC	Maleimide derivatives of alkynes followed by azido bearing Tn antigen, ³⁴ maleimide derivatives of thiol-reactive chromophores ^{39,40}
	PAG (S123C mutant)	Potassium ferricyanide-mediated oxidative coupling	o-aminophenols or o-catechols ⁴¹

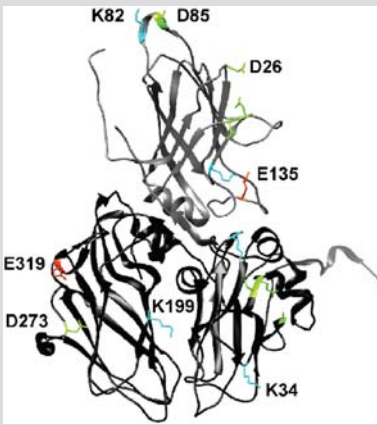
Q β

	K2, K13, K16, N-terminus	Acylation/CuAAC	Tn antigen, ⁴² bovine serum albumin, ⁴³ fluorescein, ⁴³ triple-sulfated ligand, ⁴⁴ AF 488, ⁴⁵ AF 568, ⁴⁶ human holo-transferrin, ⁴⁶ poly(2-oxazoline), ⁴⁷ PEG-C ₆₀ , ⁴⁸ oligomannosides, ⁴⁹ LacNAc, ⁵⁰ BPC sialic acid, ⁵⁰ Gd(DOTA) ⁵¹
	M16HPG	CuAAC	Oligomannosides ⁴⁹
	T93AHA	CuAAC	RGD-PEG, ⁵² biotin ⁵²

P22

	S39C	EDC/NHS	Mn porphyrin ⁵³
		ATRP	AEMA ⁵⁴
	K118C	ATRP	THMMA ⁵⁴
		Thiol-maleimide	Bortezomib ⁵⁵
		CUAAC	DTPA-Gd ⁵⁶
	T183C, M338C, C-terminus	Thiol	MIANS, ⁵⁷ HIV-TAT CPP, ⁵⁸ mCherry ⁵⁹

CPMV

	K34, K38, K82, K99, K199	CUAAC	Peptides, ^{60,61} folic acid, ⁶² fluorescein-PEG, ^{63,64} transferrin, ⁶³ GD-DOTA ⁶⁵
		EDC/NHS	OG 488, ⁶¹ AF 568, ⁶¹ AF 555, ⁶¹ AF647, ^{66,67} PEG, ^{66,67} ferrocene, ⁶⁸ peptides ⁶⁹
	R82C, A141/163C	Thiol-maleimide	Proteins ⁷⁰

AEMA, Aminoethyl methacrylate; AF, Alexa Fluor; CuAAC, copper-catalyzed azide alkyne 1,3-dipolar cycloaddition; MIANS, 2-(4'-maleimidylanilino) naphthalene-6-sulfonic acid; PEG, Poly(ethylene glycol); RGD, arginyl-glycyl-aspartyl; THMMA, tris(hydroxymethyl)methylacrylamide.

as a means of controlling uptake. This ability to further functionalize VLPs allows researchers to go one step further than simply improving capsid stability through the use of groups like polyethylene glycol (PEG); it allows the design of smarter delivery vessels that can be targeted to specific cell types^{89,90} or introduce stimuli responsive release.^{91,92} Recently, more focus has been placed on understanding the immunogenicity^{42,93–95} of these particles and employing them to treat aggressive diseases.^{14,15} Their application as vaccines is plausible considering their small size and ability to illicit an immune response via their repetitive epitope display⁹⁵ that also shows promise as an innate adjuvant. With these characteristics in mind, this chapter highlights the advantages VLPs offer to biomedical applications. Each of the aforementioned characteristics affords VLPs the ability to overcome limitations associated with current state-of-the-art technologies. Because most research has been focused on developing VLPs for imaging, sensing, and drug delivery applications, overviews of these areas will be presented to demonstrate the characteristics of VLPs that provide specific advantages over traditional systems. It is worth mentioning that VLPs are relatively easy for the nonbiologist to produce and require only a small investment in equipment. A number of detailed protocols, including video protocols, exist and are worth reviewing.^{96–99}

11.2 Imaging applications

VLPs are biocompatible macromolecules that bring many advantages to imaging applications. The monodisperse and multivalent coat proteins that make up the VLP contain repeating functional handles from lysine, cysteine, aspartate, glutamate, and tyrosine residues that can be used in bioconjugation reactions to attach imaging agents to the virus.¹⁰⁰ The monodispersity of the coat proteins allows for uniformly spaced attachment of many imaging agents to each VLP for improved resolution.¹⁰¹ Furthermore, the multivalency of the coat proteins allows for the utilization of a second functional handle that can be used to attach a targeting ligand orthogonally for improved localization of the imaging agent in a desired region of the body.⁸⁰ In certain contexts, these attributes make VLPs attractive alternatives to hard nanoparticles, which tend to bioaccumulate and have limited surface chemistry for functionalization.¹⁰² They also offer atomistically precise surfaces for functionalization in contrast to polymeric systems, which are polydisperse and have spatially disordered functional handles. The proteinaceous makeup of the VLP can help make conjugated synthetic and inorganic imaging agents more biocompatible improving the ability of these agents to translate into *in vitro* and *in vivo* studies.¹⁰³ Additionally, VLPs come in different shapes and sizes that

can be selected for longer retention times which allow for higher accumulation in the desired area and can extend imaging time.¹⁰³ For instance, isotropic VLPs can endure longer circulation times, whereas anisotropic VLPs can avoid phagocytosis by macrophages. Additionally, larger VLPs have been shown to accumulate in tumors because of the enhanced permeation and retention (EPR) effect. These characteristics make VLPs good candidates for next-generation imaging applications.

In this section, we will highlight VLP-based imaging platforms focusing on fluorescence and magnetic resonance imaging (MRI). These two areas of imaging specifically have drawn the interest of many research groups who work with VLPs. Through their work, they have been able to increase the brightness and localization of fluorescent probes as well as increase the relaxivity rates of commonly used lanthanide-based contrast agents. A few examples of these advances in imaging technology are discussed in the following section.

11.2.1 Fluorescent and optical probes

One of the earliest applications of VLPs in biotechnology was to use them as fluorescent nanoparticles for cell imaging. By attaching fluorescent dyes to the multivalent surface of a VLP, the local density of the small molecule fluorophores creates brighter imaging agents for higher-resolution imaging.¹⁰⁰ Furthermore, by reacting at specific sites on the protein that are physically separated in space, collisional quenching between adjacent fluorophores can be avoided, thereby improving the brightness of the nanoparticle. Small molecules can be conjugated to VLPs through a variety of high-yielding bioconjugation reactions.¹⁰⁰ For instance, EDC/NHS chemistry can be used to attach small molecules to lysine residues, diazonium coupling for tyrosine residues, carbodiimide chemistry for glutamate residues, and maleimides for cysteine residues.¹⁰⁴ More recently, “rebridging reactions” on VLPs have made the disulfide bridge an amenable functional handle.¹⁰⁵

Some of the first work done on creating fluorescent VLPs for *in vitro* imaging applications came out of the Manchester group. Lewis et al. attached¹⁰⁶ 120 Alexa Fluor 555 molecules to each CPMV (cowpea mosaic virus) without any self-quenching of the fluorophores. This conjugate was determined to be much brighter compared with conventional imaging agents made from polystyrene nanospheres carrying the same dye—demonstrating a practical benefit over polymeric systems. Because the multivalency of the VLP coat proteins allow for the attachment of a dye to one functional handle and a targeting ligand to another,¹⁰⁷ it is possible to make bright targeted probes using two-relatively straightforward chemical reactions. For example, Carrico et al. demonstrated¹⁰⁸ that

M13 phage could be modified with both Alexa Fluor 488 and antibody fragments to epidermal growth factor receptor (EGFR) or human epidermal growth factor receptor 2 (HER2) to target imaging of breast cancer cells for diagnostic applications (Fig. 11.1). *In vitro* studies demonstrated the selective uptake of the targeted VLPs in cells expressing EGFR or HER2 by flow cytometry as well as localized fluorescence of the VLP conjugate in these cells by confocal microscopy. This work provides a very strong example of how targeted VLPs can be used in high-resolution fluorescence imaging.

VLPs come in different shapes, sizes, and charges that can be selected for and employed as a targeting function for the imaging agent. For instance, positively charged VLPs encourage cell uptake;⁶⁹ larger VLPs are more likely to accumulate in tumors due to the EPR effect,¹⁰⁹ and elongated VLPs avoid phagocytosis by macrophages.¹¹⁰ Bruckman et al. utilized³² the elongated rod shape of the plant viral nanoparticle, tobacco mosaic virus (TMV), to target vascular cell adhesion molecule (VCAM)-1 for imaging of atherosclerosis. The elongated shape (300 × 18 nm) of the VLP enhances the ability of the nanoparticle to bind to the flat walls of the arteries displaying VCAM-1.

As this technology matures, new chemistries are demanded to increase the number of fluorophores and conjugate handles for targeting ligands to help increase the scope and utility of VLPs. For instance, recent work from Chen et al. established¹⁰⁵ a high-yielding method to conjugate a variety of dibromomaleimide handles to the disulfide bonds that bridge the pores of the VLP Q β . Disulfides are typically structurally vital to protein tertiary structure, but Chen's approach effectively retained the covalent bond character. Furthermore, the resulting five-membered ring that bridges the disulfide is itself fluorescent. The resulting dithiomaleimide cores are modestly bright yellow fluorophores, which allow the conjugates to be imaged *in vitro* (Fig. 11.2) while concurrently allowing for additional functional handles or PEG chains.

In conclusion, the conjugation of fluorescent dyes to the VLP capsid can improve the resolution of fluorescent imaging due to the high loading capabilities and monodisperse display of the dye on the VLP. Similarly, the same characteristics of the VLP capsid can be exploited to obtain high contrast MRI. In the next section, we will discuss some of the advantages VLPs offer for MRI contrast agents.

11.2.1.1 Contrast agents

Contrast-enhanced MRI is an imaging technique that uses contrast agents to greatly exacerbate the relaxation of water molecules compared with their environment making them appear either very bright (T₁ contrast) or very dark (T₂ contrast). Paramagnetic contrast agents, such as gadolinium (Gd³⁺) ions, are commonly used to increase contrast (T₁)

by altering relaxation times.¹¹¹ How well a given contrast agent works is related to a number of physical phenomena, one of which can be altered by simply attaching the small molecule to something very large. Large macromolecules, like VLPs, have slow rotational dynamics in solution compared with small molecules.^{112–114} Quite generally, though exceptions exist, there is an inverse relationship between the rate of rotational dynamics (rotational correlation time) and the relaxation rate (relaxivities) denoted as r_n , $n = 1, 2$ for T₁ or T₂ of a contrast agent. Consequently, one way to improve the overall ability of a given small molecule contrast agent is to stick it onto something very big. One of the first examples of VLPs used to augment T₁ contrast was done by Qazi et al., who attached an impressive 1900 chelated Gd³⁺ ions to P22 to achieve high relaxivity values, specifically $r_{1,\text{ionic}} = 21.7$ mM/s and $r_{1,\text{particle}} = 41,300$ mM/s at 298 K, 0.65 T (28 MHz).⁵⁶ This improves the localization density of the contrast agents and lowers the threshold detection limit of imaging agents used in MRI.¹¹⁵

Additionally, the large size of VLPs can be harnessed to slow the tumbling rate of contrast agents to improve MRI resolution. Prasuhn et al. conjugated⁵¹ 223 Gd(DOTA) molecules to the exterior surface of CPMV and 153 to the exterior surface of Q β . This resulted in a doubling of the relaxivity of Gd as compared with the FDA-approved Magnevist MRI contrast agent. The improved relaxivity is attributed to the limited rotational movement and diffusion associated with large VLPs. Similarly, Liepold et al. utilized¹¹¹ the large size of the 28 nm cowpea chlorotic mottle virus (CCMV) to conjugate up to 360 Gd(DOTA) to the exterior lysines on each capsid for a slowed tumbling rate and improved r_1 and r_2 relaxivities as compared with free gadolinium ions (Fig. 11.3).

Another method to improve the effectiveness of contrast agents is to incur rigidity within the chelated Gd³⁺. This can be achieved by conjugating Gd(DOTA) to a functional handle on a VLP. Bruckman et al. found³³ that Gd(DOTA) conjugated to the tyrosine residues on the surface of TMV-improved relaxation threefold compared with free Gd(DOTA) and twofold when conjugated to the glutamate residues on the interior surface (Fig. 11.4). According to the authors, conjugation to the tyrosine residues offered higher rigidity compared with the more flexible carboxylic acids from the glutamate residues, which correspondingly enhanced the Gd(DOTA) relaxivity, though an alternative explanation might also include the slower water diffusion through the internal pore of TMV.

The multivalent functional handles on the VLP also allow for the conjugation of a targeting ligand for localization of the contrast agents in a specified region of the body. Hu et al. created¹¹⁶ a TMV bimodal imaging agent that targeted prostate cancer cells. To do so, Cy7.5 and Dy(DOTA) were conjugated to the interior glutamate

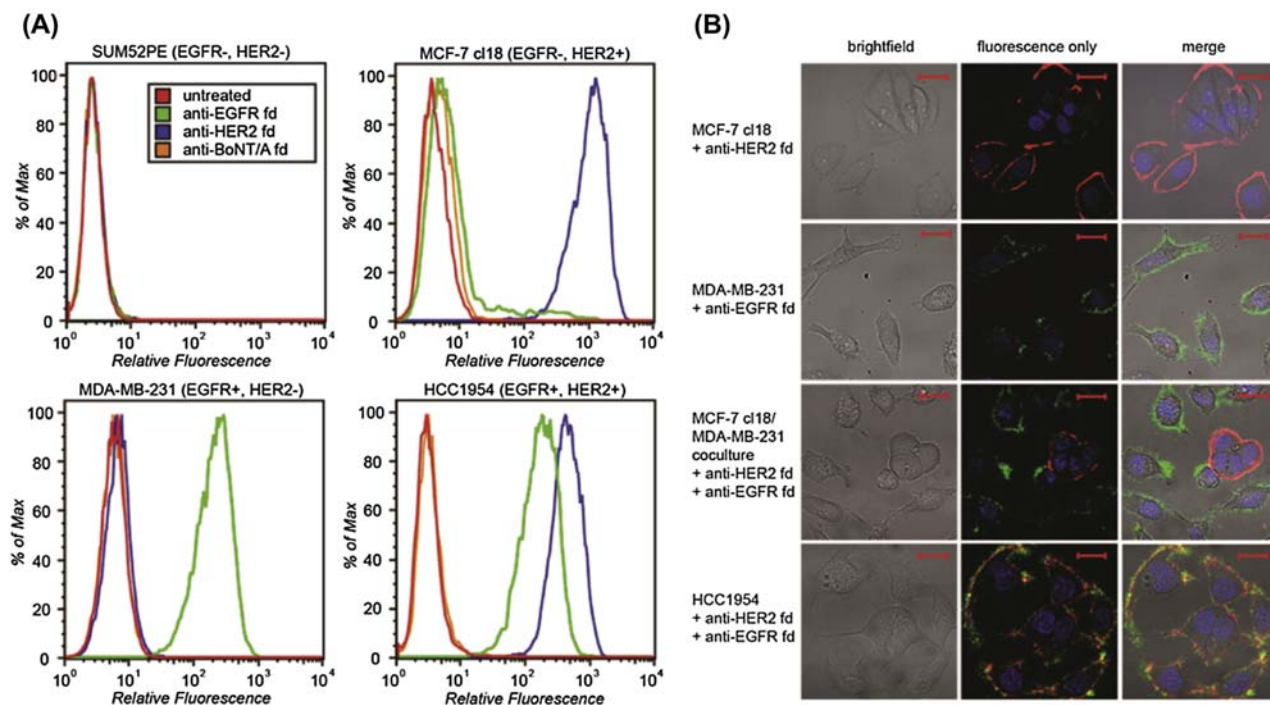


FIGURE 11.1 The N-terminus of phages was conjugated to fluorophores. The phage-displayed antibodies targeted breast cancer cells by recognizing epidermal growth factor receptor (EGFR) or human epidermal growth factor receptor 2 (HER2). It is shown in (A) that the phage–fluorophore conjugate was able to specifically recognize the EGFR and HER2 epitopes as determined by flow cytometry. It is shown in (B) that the phage–fluorophore conjugate targets breast cancer cells with the EGFR or HER2 for visualization by confocal microscopy. *Reproduced with permission from Carrico ZM, Farkas ME, Zhou Y, Hsiao SC, Marks JD, Chokhawala H, Clark DS, Francis MB, N-Terminal labeling of filamentous phage to create cancer marker imaging agents. ACS Nano 2012;6(8):6675–6680.*

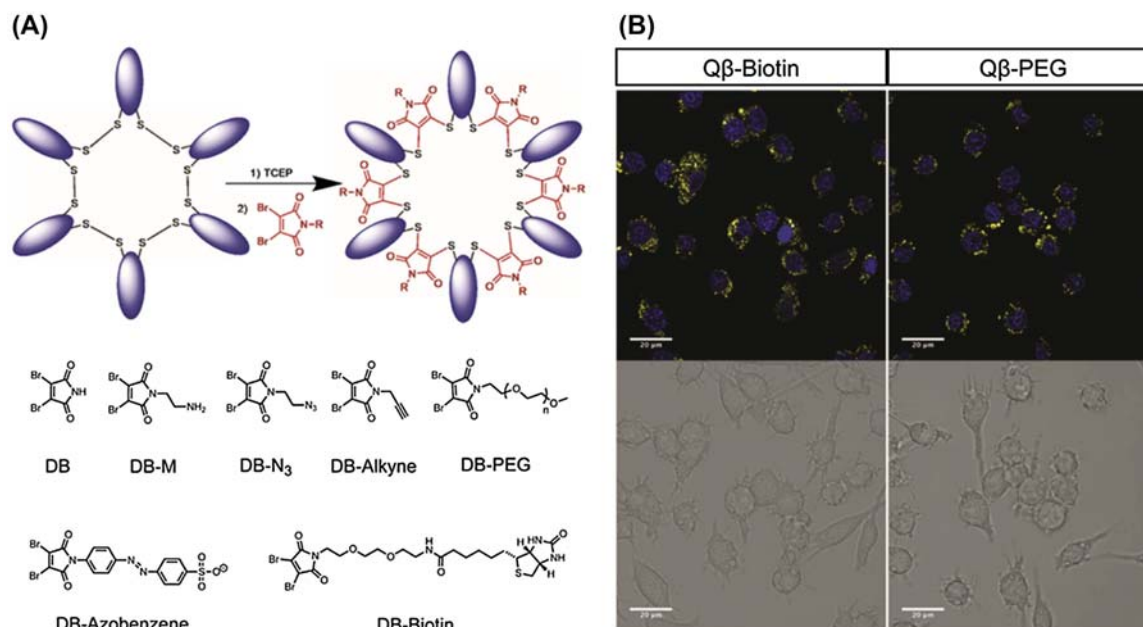


FIGURE 11.2 (A) Synthesis of Q β –maleimide conjugates with a variety of functional groups. (B) *In vitro* fluorescence imaging by confocal microscopy of biologically relevant Q β conjugates. The yellow fluorescence is from the five-membered dithio-maleimide rings created in the bioconjugation reaction. *Reproduced with permission from Chen Z, Boyd SD, Calvo JS, Murray KW, Mejia GL, Benjamin CE, Welch RP, Winkler DD, Meloni G, D’Arcy S, Gassensmith JJ. Fluorescent functionalization across quaternary structure in a virus-like particle. Bioconjug Chem 2017;28(9):2277–2283.*

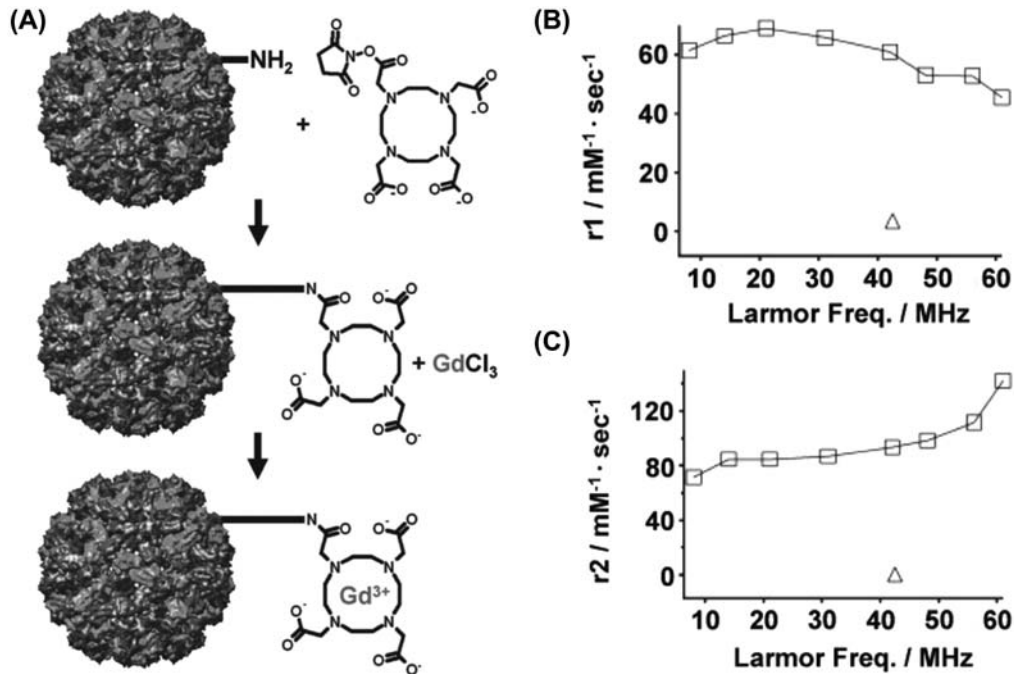


FIGURE 11.3 The relaxivities of “free” gadolinium ions (GdCl_3) are compared with gadolinium ions conjugated to the VLP cowpea chlorotic mottle virus. (A) shows the attachment of Gd. The triangles represent the free Gd, and the squares represent the conjugated Gd. (B) shows the r_1 values, and (C) shows the r_2 values. It is clear from both (B) and (C) that the conjugated gadolinium ions have higher relaxivities suggesting that the slowed tumbling rate improves the efficacy of the contrast agent. *Reproduced with permission from Liepold L, Anderson S, Willis D, Oltrogge L, Frank JA, Douglas T, Young M. Viral capsids as MRI contrast agents. Magn Reson Med 2007;58(5):871–879.*

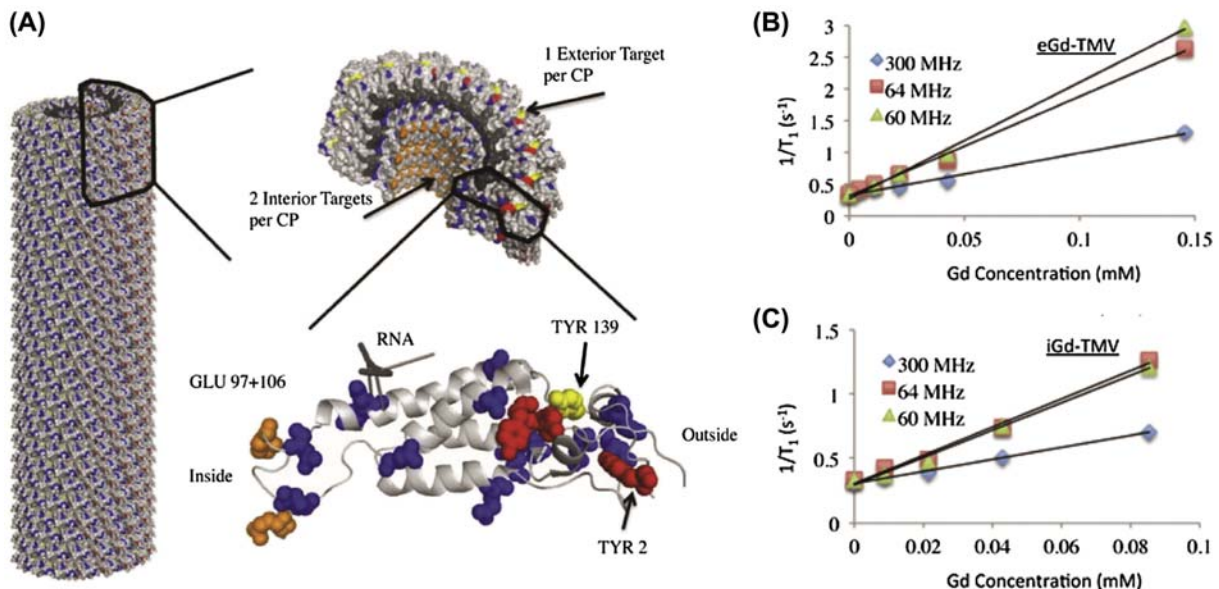


FIGURE 11.4 Gd(DOTA) is attached to the exterior tyrosine residues to form (eGd-TMV) and interior glutamate residues to form (iGd-TMV). The attachment sites are highlighted in (A). At 60 MHz, the slope of eGd-TMV shown in plot (B) gives an r_1 value of 18.4 mM/s which is threefold higher than free Gd(DOTA) (4.9 mM/s at 60 MHz). At 60 MHz, the slope of iGd-TMV shown in plot (C) gives an r_1 value of 10.7 mM/s which is twofold higher than free Gd(DOTA). These plots suggest incurred rigidity of the Gd(DOTA) after conjugation to the VLP with the highest rigidity and relaxation values when conjugated to the exterior tyrosine residues. *Reproduced with permission from Bruckman MA, Hern S, Jiang K, Flask CA, Yu X, Steinmetz NF. Tobacco mosaic virus rods and spheres as supramolecular high-relaxivity MRI contrast agents. J Mater Chem B 2013;1(10):1482–1490.*

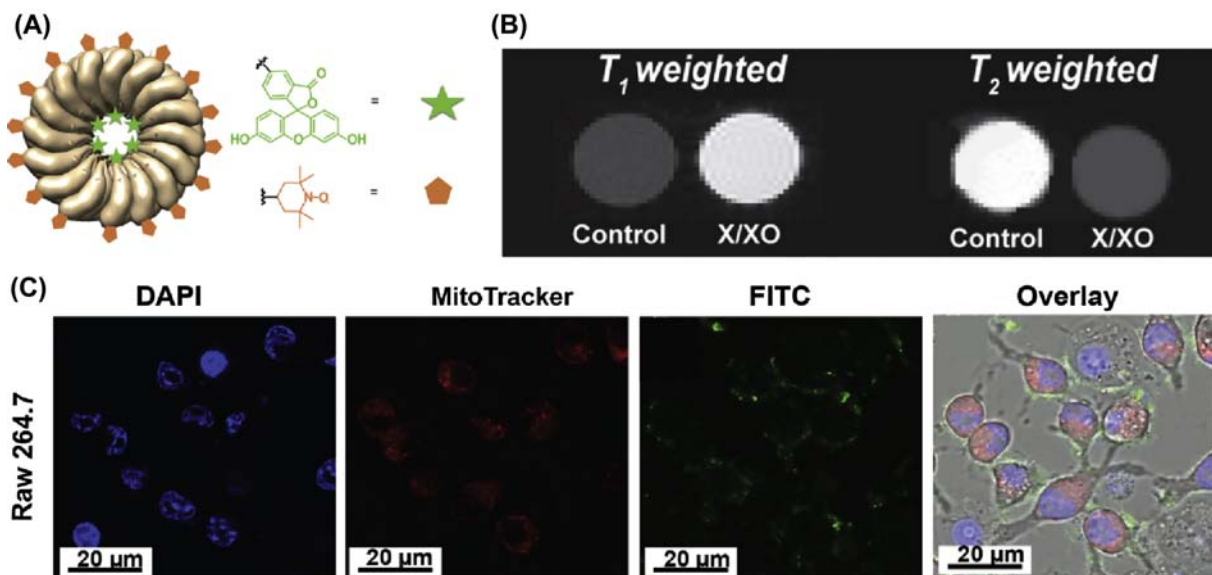


FIGURE 11.5 The virus-like particle tobacco mosaic virus (TMV) is shown to work as both an MRI contrast agent and a fluorescent probe. (A) TEMPO is conjugated to the exterior surface of TMV and works as a contrast agent for MRI imaging (orange pentagon). FITC is conjugated to the interior surface of the TMV and is used for fluorescent imaging (green star). Together the TMV conjugate can be used in both MRI (B) and fluorescence imaging (C) applications. *Reproduced with permission from Dharmarwardana M, Martins AF, Chen Z, Palacios PM, Nowak CM, Welch RP, Li S, Luzuriaga MA, Bleris L, Pierce BS, Sherry AD, Gassensmith JJ. Nitroxyl modified tobacco mosaic virus as a Metal-free high-relaxivity MRI and EPR active superoxide sensor. Mol Pharm 2018;15(8):2973–2983.*

residues of TMV for NIR imaging and MRI. PEG and DGEA were conjugated to the tyrosines on the exterior surface for a biocompatible probe that specifically images prostate cancer.

Another bimodal imaging agent using TMV was designed by Dharmarwardana et al. in which FITC was conjugated⁷⁶ to the exterior tyrosine residues for fluorescence imaging and TEMPO was conjugated to the interior glutamates for MRI (Fig. 11.5). Uniquely, this MRI probe is also a superoxide sensor as the organic radical contrast agent, TEMPO, is reduced in *in vitro* and *in vivo* environments into an MRI silent state, but upon oxidation by superoxide, it functions as a “turn on” MRI sensor. This allows the sensor to “turn on” in T_1 and T_2 weighted imaging. The reduced state is MRI inactive, showing up as dark (T_1) or light (T_2), while the oxidized state is MRI active. This sensor can be used to show areas of high concentrations of superoxide, which exist in certain injury states. In the following section, the use of VLPs in sensor applications is discussed.

11.3 Virus-based sensors

Development of biological detection systems has received a considerable amount of attention in the biomedical field owing to its vital importance in clinical diagnosis and treatment. However, many available biosensors such as enzyme, cell-based, electrochemical, and color-based sensors suffer from limited sensitivity, selectivity, reliability,

simplicity, and stability to detect and identify biological targets with high levels of certainty.^{116–118} Accordingly, there is a pressing need for the invention of advanced biorecognition probes to overcome these challenges. VLPs have been employed as a sensing platform, thanks to their ease of synthetic and genetic modification to their coat proteins, which can be used to enhance the binding affinity for specific targets to solve selectivity and sensitivity problems. Moreover, by strategically engineering or functionalizing the multivalent surface of a viral capsid, these particles are able to detect multiple analytes such as proteins, DNA, virus, antibodies, etc. Because VLPs are monodisperse, they allow the attachment of precise and high amounts of target analytes to the capsid giving high accuracy, rapid detection, and significant response to signal amplification. In the following sections, we will review some examples of different virus-based sensors.

11.3.1 Enzyme-based biosensors

An enzyme-based biosensor is an analytical tool that detects changes in the enzymatic activity of a substrate. Therefore, the presence of high amounts of enzyme as a molecular recognition element can enhance response signal toward the target molecule, resulting in a highly sensitive sensor with a short detection time. Moreover, using highly specific enzymes toward the desired target allows for enhanced selectivity of the sensor. At present, there are several examples of selective and sensitive enzyme

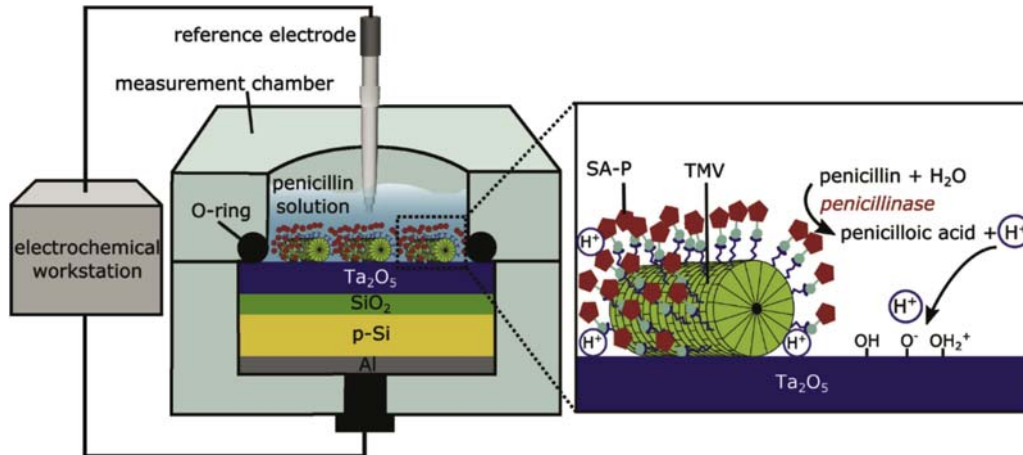


FIGURE 11.6 Schematic structure of modified tobacco mosaic virus (TMV) and penicillin biosensor. TMV modified with biotin groups to conjugated penicillinase—streptavidin (SA-P). The sensor is built up by immobilization of functionalized TMV on a pH-sensitive Ta_2O_5 gate EIS. The probe can detect hydrolysis of penicillin through monitoring the changes in hydrogen ion concentration (pH) near the surface of Ta_2O_5 . The result is a change in the surface charge of Ta_2O_5 gate and the depletion capacitance in the silicon, which leads to changes in the overall capacitance of the EIS biosensor. Reproduced with permission Poghossian A, Jablonski M, Koch C, Bronder TS, Rolka D, Wege C, Schoning MJ. Field-effect biosensor using virus particles as scaffolds for enzyme immobilization. *Biosens Bioelectron* 2018;**110**, 168–174.

biosensors, such as the glucose biosensor that generally uses glucose oxidase (GO) to catalyze oxidation of β -D-glucose.¹¹⁹ Although these sensors are selective, they suffer from instability, high detection limits, and high production costs.¹²⁰ These limitations result from poorly absorbed enzymes, environmental changes (pH and temperature), low enzyme activity, and low signal detection.

To address these problems, there are several reports on integration of available probes with VLPs.^{121–124} A recent example is coupling,¹²⁵ the enzyme modified TMV to a Pt sensor chip for amperometric detection of glucose. For this purpose, a streptavidin-conjugated glucose oxidase ([SA]-GOD) complex was immobilized on the surface of biotinylated TMV through bioaffinity binding. The functionalized TMV was loaded on the Pt electrode which caused a significant increase in enzyme density on the surface of the sensor chip. The result is higher glucose signal, lower detection limit, and high enzyme activity.

Additionally, VLPs can be used as a specific sensing platform for β -galactosidase. Nanduri et al. has shown that⁷⁷ the filamentous bacteriophage IG40 has high binding affinity to galactosidase which can be used for sensitive and specific detection of this enzyme. They immobilized IG40 on a gold surface of SPR SPREETATM sensor chip and compared the sensor performance with an F8-5 as a control phage (nonspecific to β -gal). Their data showed a 10-fold enhancement in detection response compared with control phage.

Additionally, the surface of VLPs exposes thousands of identical binding sites that permit the attachment of a large number of enzymes to the viral capsid in a spatially controlled manner. Conjugated enzymes maintain their structure and catalytic activity, both of which are required for a sensitive

enzyme-based probe. One example of the conjugation of enzymes to a VLP for the development of a probe was shown by Poghossian et al. In this study, they demonstrated¹²⁴ the strong immobilization of penicillinase enzyme on TMV via biotin and streptavidin—penicillinase binding affinity. The modified TMV was loaded on Al-p-Si- SiO_2 - Ta_2O_5 as an electrolyte insulator semiconductor to build a highly sensitive and stable biosensor (Fig. 11.6). The modified sensor is able to detect penicillin concentrations in the range of 0.1–10 mM with a 50 μM lower detection limit.

VLPs have great potential for successful integration with other sensors owing to their desirable properties such as coupling biological elements like enzymes, high thermal and chemical stability, and lack of toxicity. This will help with the emergence of novel sensors with promoted performance like the analyte detection over low concentration range, high specificity, and stability.

In addition to use of VLPs in developing the enzyme-based sensors, they can be applied as a color-based probes and use different optical techniques (fluorescence spectrometry, UV/Vis, chemiluminescence) for biomolecular interaction analysis and specific detection and identification of a variety of biological analytes. In the following section, we will show the examples of VLPs as a colorimetric sensor.

11.3.2 Colorimetric biosensors

Colorimetric biosensors produce human and machine-readable color changes in response to biological analytes. General drawbacks of these sensors tend to be poor selectivity and relatively low sensitivity, which limit their clinical applications; therefore, there is a need for new

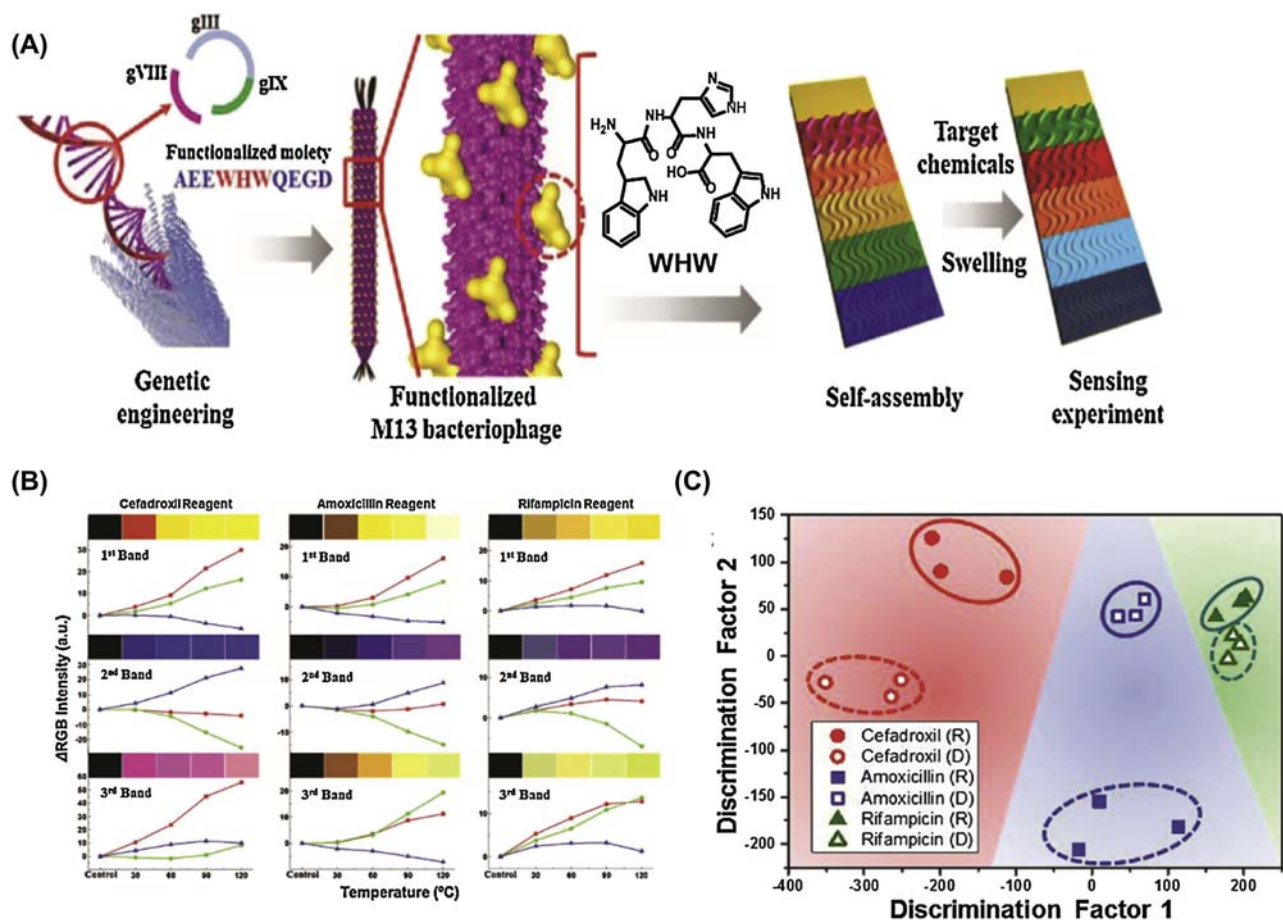


FIGURE 11.7 Schematic illustration of colorimetric sensor composed of filamentous M13 modified with WHW peptide. (A) The self-assembly properties of M13 has been used to make liquid crystalline thin films by the pulling technique. (B) The RGB signal intensity was changed in the presence of different antibiotics at different temperatures owing to changes in the M13-based bundle nanostructure. (C) Principal component analysis (PCA) was used to show discrimination ability of the sensor for different antibiotics (cephalosporin, penicillin, and rifampin). *Modified with permission from Moon JS, Park M, Kim WG, Kim C, Hwang J, Seol D, Kim CS, Sohn JR, Chung H, Oh JW, M-13 bacteriophage based structural color sensor for detecting antibiotics. Sens Actuators B Chem 2017;240, 757–762.*

architectures to enhance sensitivity toward bioanalytes. VLPs can be engineered chemically and genetically to promote intrinsic affinity toward a specific analyte. For example, Oh and coworkers introduced⁷⁸ a selective and stable colorimetric probe for the detection of different types of antibiotics by using the self-assembly properties of a genetically engineered nonlytic M13 VLP. In this study, an M13 was functionalized with the WHW peptide to have 1000 copies of tryptophan (W) histidine (H) tryptophan (W) sequences which can act as a receptor for antibiotics. Target binding causes the quasi-ordered bundles of phage matrices to swell or shrink, which induces a change in the optical scattering properties on the chip surface following interaction with different target antibiotics (Fig. 11.7). This scattering of light results in an apparent color, even though no chromophores are present.

For early disease diagnostics, there is critical need for tools to sense and measure different biological molecules, proteins, and biomarkers on cancerous cells. To date,

several colorimetric sensors such as enzyme-linked immunosorbent assay (ELISA) and cell-based ELISA (CELISA) have emerged for this purpose; however, because of the limited number of attached enzymes and high dissociation constant between antibody and antigen, their detection limit is in the nanomolar range.^{126,127} Recently, VLPs have offered several improved colorimetric sensing systems with higher response signals.^{128–131} For example, Brasino et al. improved¹²⁷ ELISA sensing performance by dually decorating a filamentous bacteriophage Fd with antibodies for specific antigen detection and horseradish peroxidase to generate an amplified colorimetric signal. In another work, Wang et al. successfully designed¹³¹ a “CELISA” using a modified TMV to detect folate receptors overexpressed on cancer cells. For this purpose, the exterior surface of TMV was modified with platinum nanoparticles as a peroxidase surrogate and folic acid as a cancer cell targeting mechanism. When the modified TMV binds to cancer cells that overexpress folic

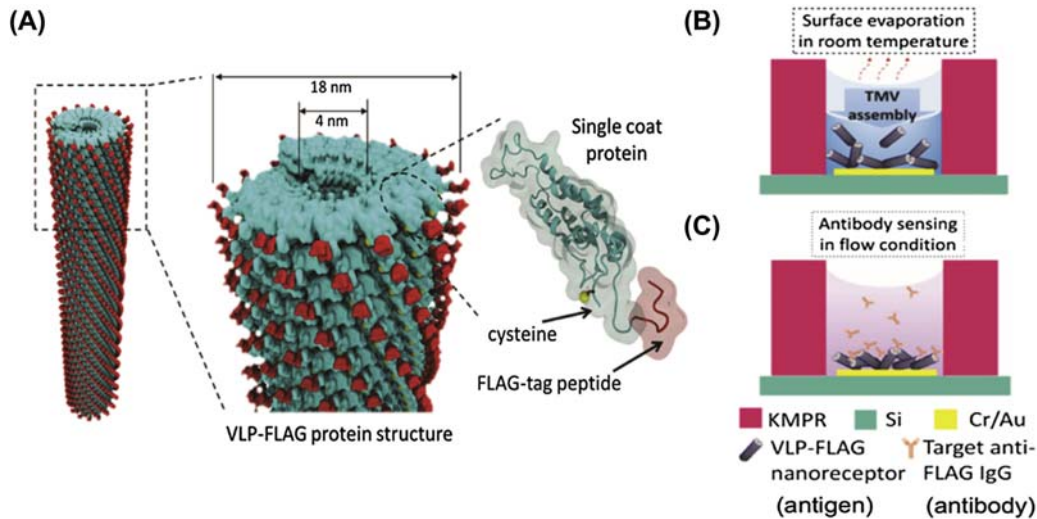


FIGURE 11.8 A) Three-dimensional schematic of modified tobacco mosaic virus (TMV) expressing cysteine residues and receptor peptide FLAG-tag. (B) Surface functionalization of TMV-FLAG. (C) Antibody detection in the sensor system. *Reproduced with permission from Zang F, Gerasopoulos K, Brown AD, Culver JN, Ghodssi R. Capillary Microfluidics-Assembled virus-like particle bionanoreceptor Interfaces for label-free biosensing. ACS Appl Mater Interfaces 2017;9(10):8471–8479.*

acid receptors, superoxide is supplemented to provide a colorimetric indicator of which cells are cancerous. Consequently, modification of VLPs has afforded a new color biosensing system that could be used for biomedical applications and diagnostics assays. Another example is an M13 bacteriophage–DNA conjugated system that has been developed¹³⁰ by Domaille et al. for protein detection. In this study, acyl hydrazone linkages were utilized for DNA sequence incorporation, which led to a strong and detectable change in absorption signal (410 nm) on interaction with IgG as a model protein. Thus, by using the phage as a sensing platform, they created a rapid and extremely sensitive tool for protein detection in the range of 0–1000 fmol.

11.3.3 Electrochemical biosensors

Electrochemical biosensors are involved in the generation or consumption of electrons over an interaction between biochemical receptors and an electrochemical transduction element. Although these sensors are usually selective and sensitive toward target biomolecules, they suffer from narrow temperature ranges, limited half-life, and high background signal. In recent decades, VLPs have received much attention for their thermal stability and robustness. Combining VLPs as a sensing receptor with analytical methods such as electrochemical methods can be a reliable way to simultaneously increase electrochemical sensor performance and improve sensor stability. For instance, Ghodssi and coworkers developed¹³² a novel electrochemical biosensor for schizophrenia analysis. In this study, they modified the surface of electrode with TMV, nickel, and gold following introduction of ssDNA

for Neuregulin-1 gene detection. The modified probe showed a high surface area with strong current change on DNA hybridization, which lead to an 8-fold increase in signal and 9.5-fold enhancement in biosensing performance.¹³²

Coating VLPs on the surface of electrodes is a way to increase the electrode surface area, thus allowing for a higher electrochemical signal, decreased signal to noise ratio, and greater sensitivity. For example, a new impedance sensor was developed¹³³ by Zang et al. that applied FLAG-tag–modified TMV on an electrode surface by capillary action and surface evaporation for label-free antibody detection. Thus, owing to the high surface to volume ratio of TMV nanotubes and several hundred available binding sites on its surface, a high peptide density could anchor to the electrode, which maximized antibody detection (Fig. 11.8).¹²⁹

Additionally, VLPs can be used as a sensing platform for biomarker and cancer cell detection. One example is the immobilization of a filamentous M13 phage on the surface of a modified Si₃N₄ chip by reacting the N terminal domain of the phage coat protein with an aldehyde group on the chip surface to make a light addressable potentiometric sensor (LAPS). Jia et al. showed¹³⁴ the sensor is able to detect human phosphatase of regenerating liver-3 (hPRL-3) at concentrations of 0.04–400 nM and mammary adenocarcinoma cell (MDAMB231) at concentrations of 0–105 cells/mL through specific binding to the phage, which had been evolved via phage display, and subsequent change of the output voltage of LAPS. Therefore, integration of bionanoreceptors with conventional electrochemical methods can be an effective strategy for improving sensor performance.

VLPs can act as a key component in different bio-sensing systems. Their potential for incorporation with different nanomaterials and analytical methods give many opportunities for scientists to expand this area of research and progress biomedical and particularly diagnostic applications. One approach is drug delivery by stimuli responsive VLPs which can show high efficacy and specificity for cargo delivery in the targeted location on sensing a particular stimulus.¹³⁵ In the following section, we will discuss this application of VLPs.¹³¹

11.4 VLPs as drug delivery vehicles

Effective drug delivery requires that the desired cargo passes several transport barriers from the site of introduction into the patient until it has reached its intended destination while avoiding off-target effects. Unfortunately, there are many barriers to successful delivery. The reticuloendothelial system hampers dosage efficacy especially if the materials have long circulation times which subsequently leads to faster clearance from the body. Additionally, cellularly targeted drugs need to permeate the membrane and avoid or survive endosomal trafficking before it releases its cargo.¹³⁶ Several nanoscale platforms are being investigated for drug delivery as nanoparticle based therapeutics as a result of their small size¹³⁷ and favorable pharmacokinetics,^{7,138} which offer solutions to many of the problems associated with conventional drug administration. Despite growing interest in their use and development, the number of FDA approved nanoparticle drugs is limited, and more than half of the formulations currently undergoing trial are liposomal.¹³⁹ These systems have been shown to suffer from rapid and dose-dependent clearance from the body^{140–144} and conflicting results on the efficacy of attaching targeting ligands.^{145,146} VLPs, on the other hand, are capable of accomplishing this task by carrying a diverse set of therapeutic cargos ranging from nucleic acids,^{130,147–151} genes,^{152,153} aptamers,^{154,155} therapeutic drugs,^{156–162} larger proteins,^{163,164} to dendrimers,^{165,166} while still being amenable to further functionalization—some have even been cleared for use by the FDA.⁷⁵ This paves a path for drug delivery to make further advancements through the utilization of a robust and tunable carrier to circumvent the issues plaguing current delivery methods.

11.4.1 Cargo loading

As discussed in previous sections, VLP geometries can play an important role in targeting and cell specificity. Because the shape of nanoparticles is known to alter their pharmacokinetics, the VLP geometry makes for a uniquely tunable parameter for drug delivery. For instance, small icosahedral nanoparticles diffuse well into tissues but have smaller cargo capacities while their larger, filamentous counterparts

are better suited for aligning with vessel walls, though they do not infiltrate cells as well. Fortunately, many viral capsids can be modified to create a more suitably sized or shaped carrier. For example, rodlike VLPs such as TMV and M13, which use their RNA to self-assemble, can be tuned to specific sizes by adjusting the length of their RNA. Icosahedral viruses, CCMV in particular, has been shown to exhibit an increase in capsid size from 27 to 30 nm linearly as the pH is varied from 5 to 7.^{167,168} Asensio et al. has gone one step further and shown¹⁶⁹ that a single amino acid change—S37P—changes the assembly of MS2 capsid proteins from 27 nm capsid with $T = 3$ symmetry to a much smaller 17 nm capsid with $T = 1$ symmetry. Further investigation on the effects of drug loading was performed by Cadena et al. to elucidate¹⁷⁰ the effects of increasing cargo size on the formation of icosahedral VLPs. They have found that varying lengths of RNA from 140 to 12,000 nt can be completely encapsulated while causing a change in capsid size. For shorter strands, the RNA is packaged into 24 and 26 nm capsids, while a single stand of RNA greater than 4500 nt is packaged by two or more 26–30 nm capsids showing that just changing the length of the structural RNA, various lengths, and sizes of VLPs can be achieved to predetermine the cargo capacity for delivery applications. Utilizing VLPs allows for increased and precise drug loading, which remedies issues with low and inaccurate dosing. Rurup et al. have demonstrated¹⁷¹ a method of predicting the loading of VLPs using teal fluorescent proteins (TFPs) and CCMV where more than 10 3 nm TFPs can be loaded inside of the 18 nm cavity of the viral capsid (Fig. 11.9). Through the use of homo-FRET, they have determined that tethering the TLPs to the capsid proteins yields more predictive and controlled loading behavior increasing the number of fluorescent proteins from 6—in the coiled coil system—to 20 dimeric units when directly bound to the CPs. This information lays some of the ground work for further progress in the use of VLPs as a drug carrier.

11.4.2 Drug delivery

Encapsulating therapeutics within a nanoparticle offers protection from rapid clearance from the body and the harsh cellular environments that would normally degrade free small molecules before reaching their target destination. The ease of functionalization of VLPs allows for the design of smarter drug delivery vehicles including stimuli responsive release. For example, work by Chen et al. utilizes⁹¹ VLP Q β , first functionalized with an azide linker on the surface exposed to NH₂, handles via EDC coupling followed by a CUAAC reaction to attach the photocleavable Dox group. The as-synthesized VLP encountered solubility issues so to remedy this, they further functionalized the surface by adding a second functional group—PEG 1K or 2K through dibromomaleimide

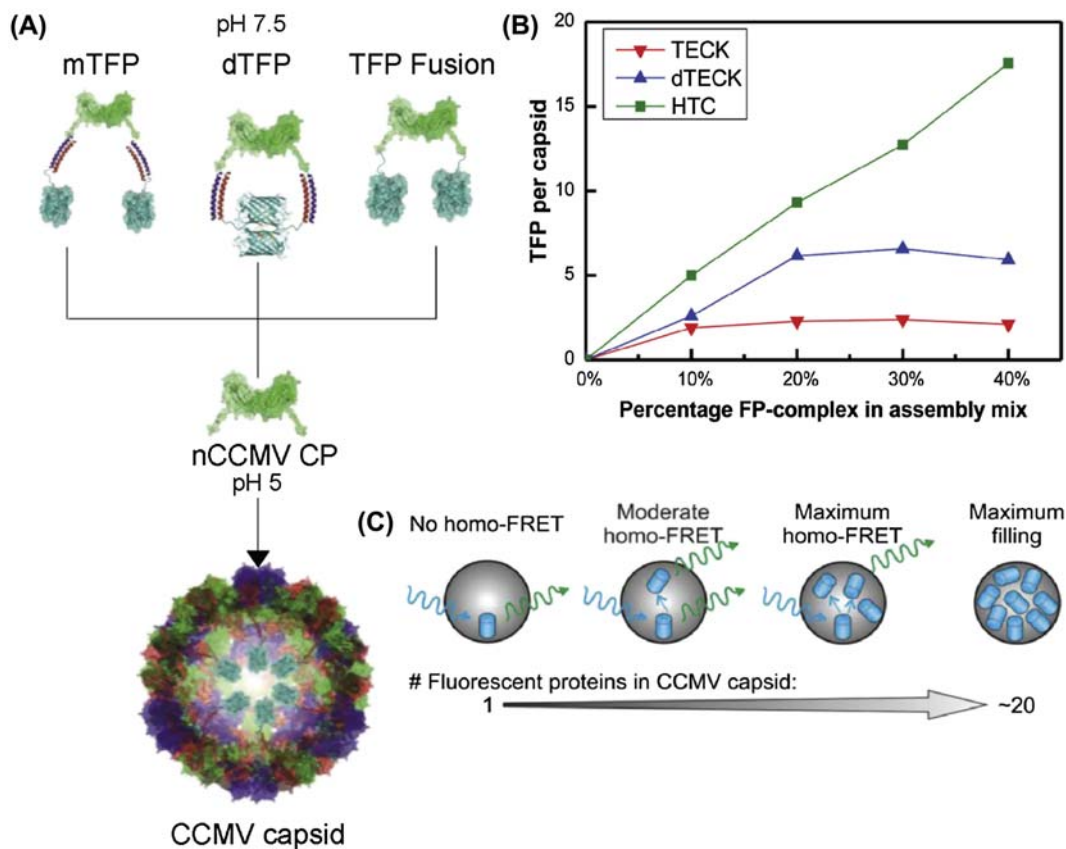


FIGURE 11.9 (A) Schematic representation of the different design principles described in this work for the rational loading of CCMV. The first approach utilizes leucine zipper like E-coils tethered to monomeric TFP (mTFP) or dimeric TFP (dTFP), which form electrostatic interactions at pH 7.5 with the complementary K-coil tethered to CCMV. The formed complex is referred to as TECK and dTECK, respectively. The second approach utilizes a genetically engineered TFP peptide linker-CCMV fusion protein, when complexed, referred to as HTC. In all cases, lowering the pH to 5.0 promotes the encapsulation of TFP cargo inside CCMV. (B) Typical capsid TFP loading as a function of percentage of complex (TECK, dTECK, or HTC) in assembly. (C) Schematic explaining how homo-FRET works. *Reproduced with permission from Rurup WF, Verbij F, Koay MST, Blum C, Subramaniam V, Cornelissen JJLM. Predicting the loading of virus-like particles with fluorescent proteins. Biomacromolecules 2014;15(2):558–563.*

chemistry. The final VLP is a soluble, low toxicity carrier that shows cytotoxicity on stimulation with UV light which cleaves the linker, activating Dox release in the cells. The Steinmetz group has also done¹⁶⁰ extensive work showing that the conjugation of molecules such as Dox can be attached and successfully delivered to cells. They have made use of the VNP CPMV decorated with covalently bound Dox on the exterior surface demonstrating that the functionalized particle in low doses is more cytotoxic than free Doxorubicin and exhibits a time-delayed release. This work has also determined that the CPMV-Dox particles get trafficked to endosomal compartments, as seen in Fig. 11.10 in HeLa cells, where the proteinaceous carrier is degraded, and the drug molecules are released into the cellular environment.

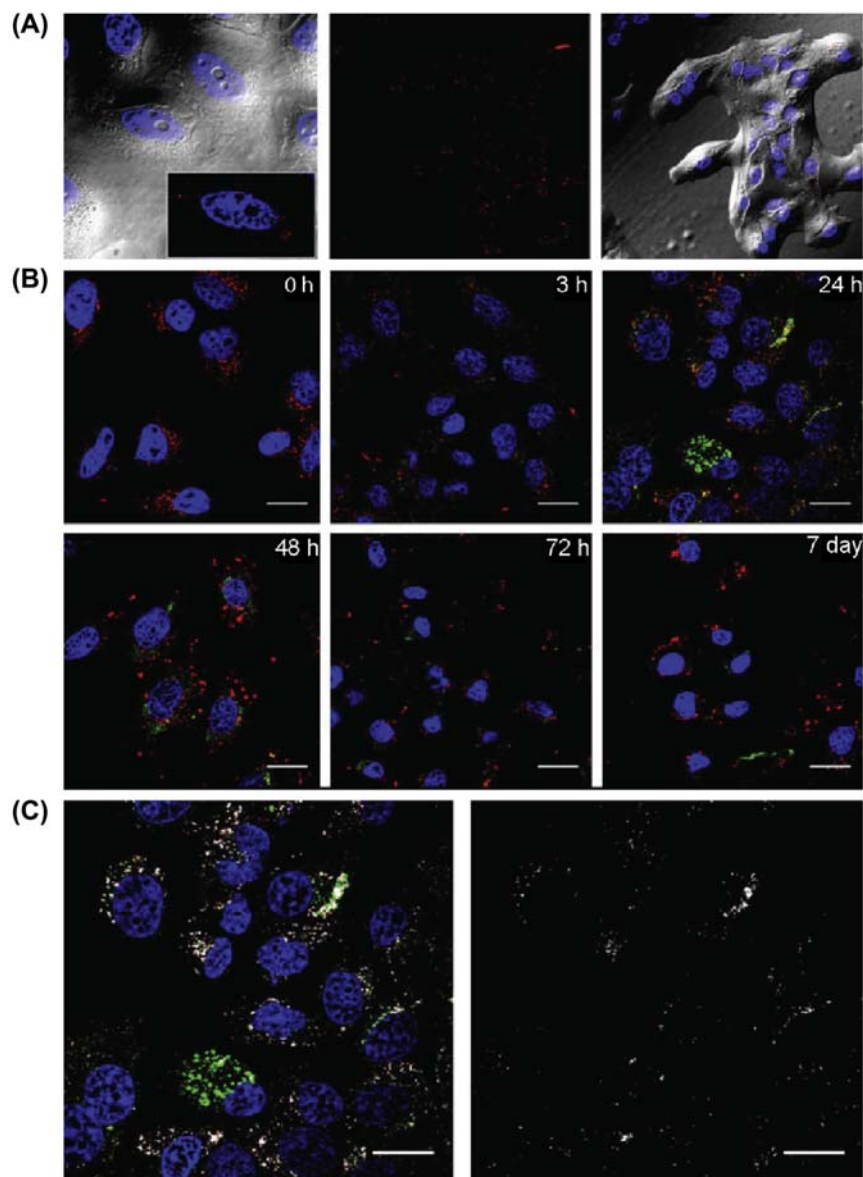
11.4.3 Targeting

The addition of a targeting functionality offers several advantages over nontargeted drugs. Mainly they consist of

reducing the side effects associated with damage to healthy tissues and enhancement of uptake into afflicted cells. Targeting can be approached in either a passive or active manner depending on the nature of the particle in use and the functionalities incorporated into its design. Passive targeting includes (1) the EPR effect, (2) approaches relying on the tumor microenvironment, and (3) intratumoral delivery.⁸⁹ The EPR effect is a phenomenon where increased permeability of the tumor vasculature is combined with poor lymphatic drainage, which makes it difficult for high molecular weight carriers to be removed from the tumor environment. EPR coupled with release based on the tumor microenvironment or an external stimulus offers some solution to healthy tissue damage and has been demonstrated across nanomedicine to be effective.⁷⁹

Many of these functionalities are applicable to VLPs that can be further modified to increase targeting specificity. Active targeting of a drug delivery system allows for the preferential accumulation into specific cells that can be selected for by a variety of tumor markers, such as small

FIGURE 11.10 (A) Imaging of CPMV-DOX in HeLa 3 h postincubation. CPMV is shown in red, nuclei are shown in blue, and DIC overlay is shown in gray. (B) Time course study showing cellular uptake of CPMV using confocal scanning microscopy; CPMV was immunostained (pseudocolored in green). Endolysosomes pseudocolored in red. Nuclei are shown in blue. Scale bar is 50 μm . (C) Colocalization analysis (white) of CPMV and Lamp-1 staining. Scale bars are 50 μm . *Reproduced with permission from Aljabali AA, Shukla S, Lomonossoff GP, Steinmetz NF, Evans DJ. CPMV-DOX delivers. Mol Pharm 2013;10(1):3–10.*



peptides and antigens as well as cell surface receptors⁴⁵ and biomarkers. These moieties have been used throughout the literature to up the chances of delivery to malignant cells—sparing the healthy ones. In an effort to increase specificity in delivery, targeting molecules have been employed such as folic acid or small peptides like cyclic RGD. For instance, Stephanopoulos et al. has constructed¹⁷² an MS2 capsid where they have attached aptamers specific to Jurkat leukemia T cells onto engineered *p*-aminophenylalanine (paF) groups followed by the conjugation of porphyrins on onto the interior cysteines that generate reactive oxygen when irradiated with blue light (Fig. 11.11). Approximately 20 aptamers were attached per capsid increasing the targeting specificity of the VLP. This

dual-modal delivery system was shown to localize only in the Jurkat cells when cocultured with other cells and successfully and selectively initiated apoptosis through photoredox ROS generation.

11.5 Vaccines

Vaccines are continually used as a method of disease treatment and prevention since their inception by making use of inactivated native viral proteins to bolster our immune systems against foreign bodies. VLPs—lacking their viral genome—produce similar immune responses to those of native, infectious diseases. The highly organized structure of the VLP surface presents several repeating amino

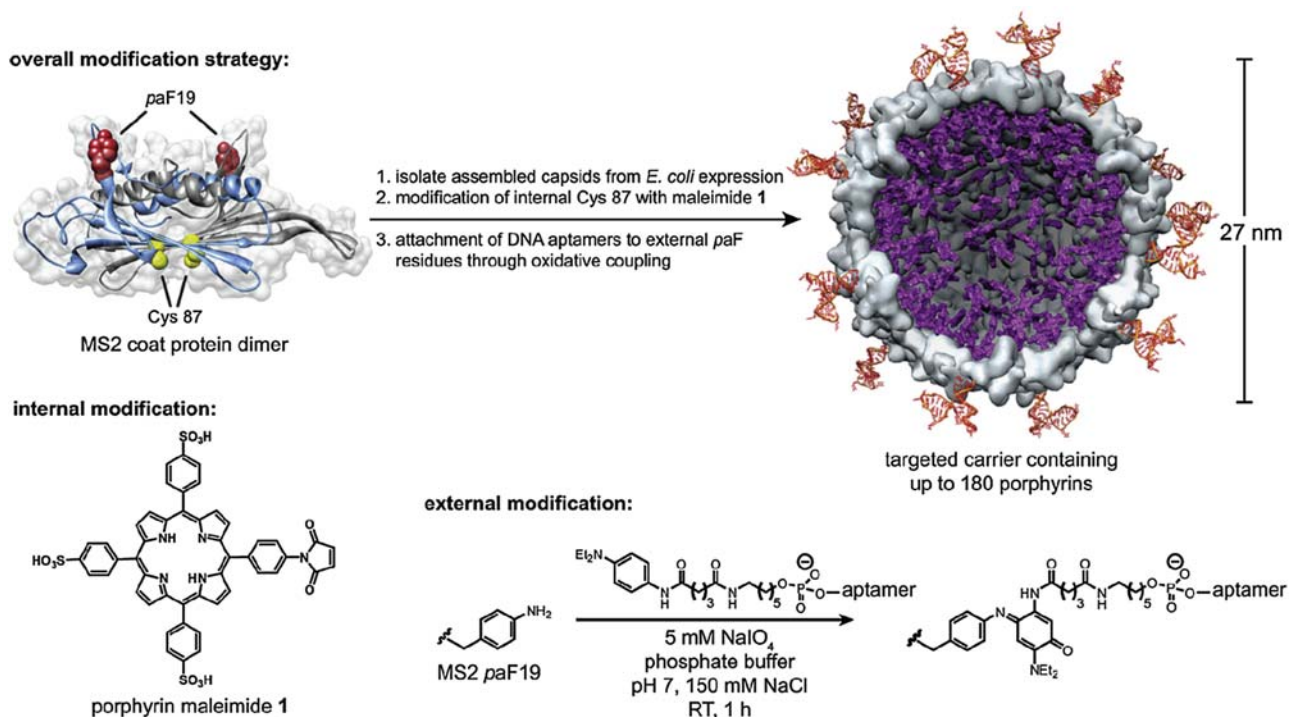


FIGURE 11.11 Construction of a multivalent cell-targeted photodynamic therapy vehicle using recombinant bacteriophage MS2. Cysteine residues on the capsid interior were modified using porphyrin maleimide 1 (rendered in purple), enabling the generation of singlet oxygen on illumination at 415 nm. Exterior *p*-aminophenylalanine (paF) residues were coupled to phenylene diamine–modified DNA aptamers to bind tyrosine kinase 7 receptors. Reproduced with permission from Stephanopoulos N, Tong, GJ, Hsiao SC, Francis MB. Dual-surface modified virus capsids for targeted delivery of photodynamic agents to cancer cells. *ACS Nano* 2010;4(10):6014–6020.

acid sequences which can cross-link B-cell receptors which, in turn, quickens the activation of antibody responses.⁹³ In addition, the encapsulated genome itself is capable of activating toll-like receptors and further eliciting an immune response with the added benefit of including a customized genetic cargo. Several VLP-based vaccines, such as human papilloma virus (HPV) and hepatitis B, are already on the market, but many more are under development.¹⁷³ The Bachmann group has conducted extensive work utilizing the Q β VLP to study its immunogenicity showing that the particle alone can transport a therapeutic while behaving as an adjuvant all in one by developing vaccines for influenza,¹⁷⁴ respiratory allergies,¹⁷⁵ and smoking cessation,¹⁷⁶ reporting as much as 100% antibody response to the injection in clinical trials. They have even gone one step further as to show the efficacy of modifying the surface of the VLP Q β with Fel d1 (Fig. 11.12), a cat allergen to induce a protective immune response without the additional threat of inducing anaphylaxis in mice.⁹⁴ In this study, to determine whether Q β –Fel d1 inhibited mast cell degeneration (which signals immune-stimulated destruction of invasive materials) in an antigen specific manner, BALB/c mice were vaccinated subcutaneously with Q β or Q β –Fel d1. When challenged 2 weeks later, mice treated with Q β –Fel d1 hardly showed an immune

response after inoculation of free Fel d1 indicating successful immune memory without adverse effects. This is an important step forward in the medical field as they have shown that VLP-based vaccines may be used as a safe, effective, and customizable method to produce vaccines.

Virus-based vaccines share some of the same problems encountered with any vaccine. Even with efficient immune responses, they rely on the longevity of the host response. In addition, use of VLPs has shown more promise than many other subunit vaccines because they are conformationally the most similar to the native virus yet are safer as they lack genetic material and thus cannot reproduce. The use of other virus-based particles such as HPV and influenza virus has sparked an interest in the further development of VLPs particularly in increasing the efficacy in these particles.

11.6 Conclusion

VLPs offer many advantages to biological applications. In this chapter, we have discussed some of the important characteristics of VLPs that can be harnessed to advance biomedical fields such as imaging, sensing, and drug delivery. There are still some issues in using VLPs in biomedical applications, in particular they are immunogenic, which means repeated exposure will change the

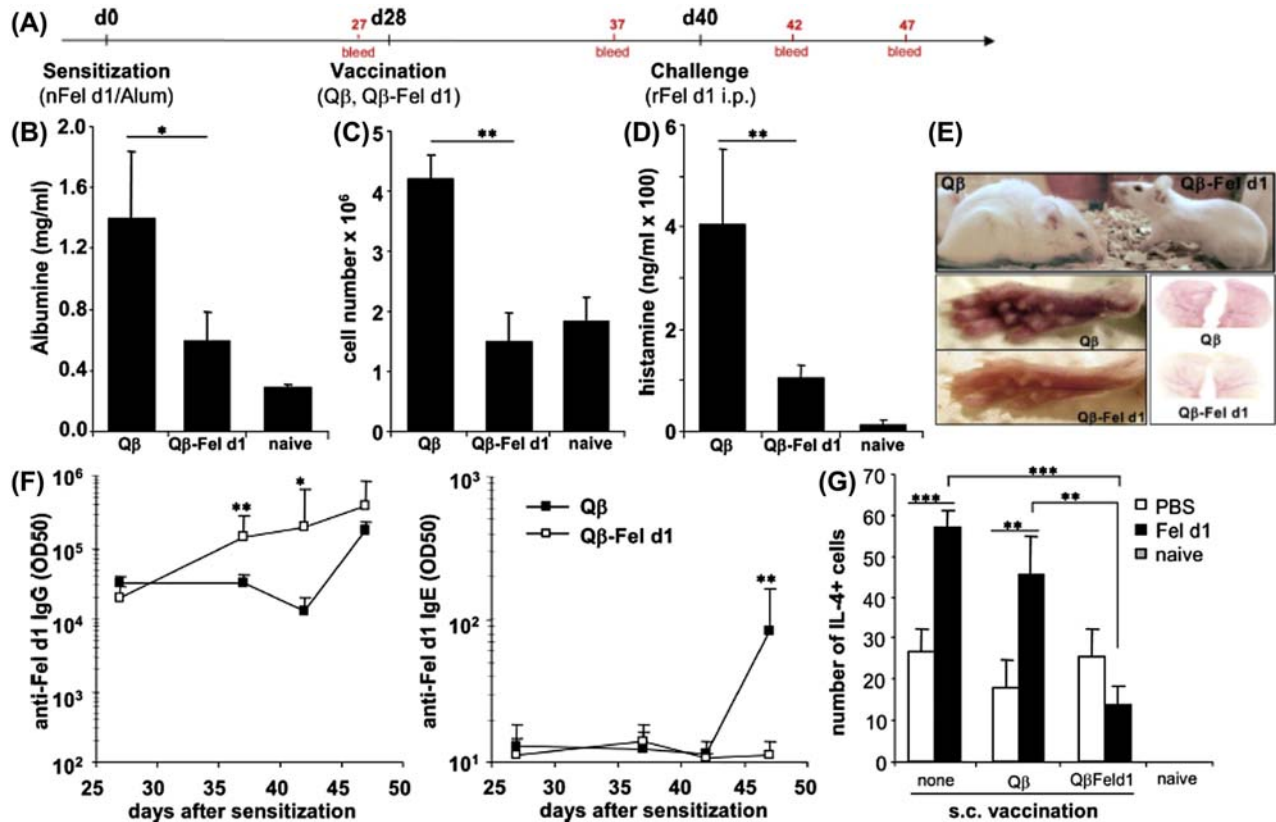


FIGURE 11.12 (A) Schematic outline of the experiment. (B–D) Mast cell activation determined by measurement of peritoneal albumin concentrations (B), peritoneal cell influx (C), and serum histamine levels (D) on antigen challenge. 40 min after intraperitoneal injection—free Fel d1 challenge. Qβ control animals displayed typical signs of anaphylactic reaction. (E) Pictures of representative animals of each experimental group, 40 min after intraperitoneal injection—free Fel d1 challenge. (F) Fel d1-specific IgG (left) and Fel d1-specific IgE (right) titers. (G) ELISPOT assays were performed 1 wk after Fel d1 challenge to determine the numbers of IL-4 producing cells per 2×10^5 spleen which are indicative of helper T-cells. *, $P < .05$; **, $P < .005$; ***, $P < .0005$. Reproduced with permission from Engeroff P, Caviezel F, Storni F, Thoms F, Vogel M, Bachmann MF. Allergens displayed on virus-like particles are highly immunogenic but fail to activate human mast cells. *Allergy* 2018;73(2):341–349.

pharmacokinetics in individual patients. This drawback is not unique to VLPs and is an issue for polymers as well.^{177,178} In context of cost, they will be more expensive than synthetic nanomaterials, though they are expressed in *Escherichia coli* in high yields, which would make their eventual scale up in a process setting relatively practical. In imaging applications, the large size of VLPs is helpful in attaching a substantial amount of dye or contrast agent, and monodisperse subunits reduce self-quenching for high-resolution imaging. The functionalizability of VLPs owed to their multivalent subunits can also be used to increase bioprobe sensitivity while maintaining stability of the conjugate. Lastly, the biocompatibility and encapsulating ability of VLPs for drug delivery helps encourage the accumulation of drugs in a specified region with reduced clearance. Because VLPs are relatively new nanocarriers, the extent of the benefits they offer for biomedical applications has yet to be realized.

References

- Chopra KL. Nanotechnology: hope or hype? *Curr Sci* 2012;102(10):1364–6.
- Mack J. Nanotechnology: what's in it for biotech? *Biotechnol Healthc* 2005;2(6):29–36.
- Wilhelm S, Tavares AJ, Dai Q, Ohta S, Audet J, Dvorak HF, Chan WCW. Analysis of nanoparticle delivery to tumours. *Nature Rev Mater* 2016;1:16014.
- Kohane DS, Langer R. Biocompatibility and drug delivery systems. *Chem Sci* 2010;1(4):441–6.
- Wilson N. Nanoparticles: environmental problems or problem solvers? *Bioscience* 2018;68(4):241–6.
- Hong H, Chen F, Cai W. Pharmacokinetic issues of imaging with nanoparticles: focusing on carbon nanotubes and quantum dots. *Mol Imaging Biol* 2013;15(5):507–20.
- Hoshyar N, Gray S, Han H, Bao G. The effect of nanoparticle size on in vivo pharmacokinetics and cellular interaction. *Nanomedicine* 2016;11(6):673–92.

8. NCI FDA Approves Talimogene Laherparepvec to Treat Metastatic Melanoma. <https://www.cancer.gov/news-events/cancer-currents-blog/2015/t-vec-melanoma>.
9. NCI Talimogene Laherparepvec. <https://www.cancer.gov/about-cancer/treatment/drugs/talimogenelaherparepvec>.
10. Lang FF, Conrad C, Gomez-Manzano C, Tufaro F, Sawaya R, Weinberg J, Prabhu S, Fuller G, Aldape K, Fueyo J. Nt-18: phase I clinical trial of oncolytic virus delta-24-Rgd (Dnx-2401) with biological endpoints: implications for viro-immunotherapy. *Neuro Oncol* 2014;**16**(Suppl. 5):v162-v162.
11. NCI Oncolytic Virus Therapy: Using Tumor-Targeting Viruses to Treat Cancer. <https://www.cancer.gov/news-events/cancer-currents-blog/2018/oncolytic-viruses-to-treat-cancer>.
12. Chesney J, Puzanov I, Collichio F, Singh P, Milhem MM, Glaspy J, Hamid O, Ross M, Friedlander P, Garbe C, Logan TF, Hauschild A, Lebbe C, Chen L, Kim JJ, Gansert J, Andtbacka RHI, Kaufman HL. Randomized, open-label phase II study evaluating the efficacy and safety of Talimogene Laherparepvec in combination with Ipilimumab versus Ipilimumab alone in patients with advanced, unresectable melanoma. *J Clin Oncol* 2018;**36**(17):1658–67.
13. Kelly E, Russell SJ. History of oncolytic viruses: genesis to genetic engineering. *Mol Ther* 2007;**15**(4):651–9.
14. Samson A, Scott KJ, Taggart D, West EJ, Wilson E, Nuovo GJ, Thomson S, Corns R, Mathew RK, Fuller MJ, Kottke TJ, Thompson JM, Ilett EJ, Cockle JV, van Hille P, Sivakumar G, Polson ES, Turnbull SJ, Appleton ES, Migneco G, Rose AS, Coffey MC, Beirne DA, Collinson FJ, Ralph C, Alan Anthony D, Twelves CJ, Furness AJ, Quezada SA, Wurdak H, Errington-Mais F, Pandha H, Harrington KJ, Selby PJ, Vile RG, Griffin SD, Stead LF, Short SC, Melcher AA. Intravenous delivery of oncolytic reovirus to brain tumor patients immunologically primes for subsequent checkpoint blockade. *Sci Transl Med* 2018;**10**(422).
15. Bourgeois-Daigneault MC, Roy DG, Aitken AS, El Sayes N, Martin NT, Varette O, Falls T, St-Germain LE, Pelin A, Lichty BD, Stojdl DF, Ungerechts G, Diallo JS, Bell JC. Neoadjuvant oncolytic virotherapy before surgery sensitizes triple-negative breast cancer to immune checkpoint therapy. *Sci Transl Med* 2018;**10**(422).
16. Hooker JM, Kovacs EW, Francis MB. Interior surface modification of bacteriophage MS2. *J Am Chem Soc* 2004;**126**(12):3718–9.
17. Kovacs EW, Hooker JM, Romanini DW, Holder PG, Berry KE, Francis MB. Dual-surface-modified bacteriophage MS2 as an ideal scaffold for a viral capsid-based drug delivery system. *Bioconjug Chem* 2007;**18**(4):1140–7.
18. Hooker JM, O'Neil JP, Romanini DW, Taylor SE, Francis MB. Genome-free viral capsids as carriers for positron emission tomography radiolabels. *Mol Imaging Biol* 2008;**10**(4):182–91.
19. Datta A, Hooker JM, Botta M, Francis MB, Aime S, Raymond KN. High relaxivity gadolinium hydroxypyridonate-viral capsid conjugates: nanosized MRI contrast agents. *J Am Chem Soc* 2008;**130**(8):2546–52.
20. Capehart SL, ElSohly AM, Obermeyer AC, Francis MB. Bioconjugation of gold nanoparticles through the oxidative coupling of ortho-aminophenols and anilines. *Bioconjug Chem* 2014;**25**(10):1888–92.
21. Capehart SL, Coyle MP, Glasgow JE, Francis MB. Controlled integration of gold nanoparticles and organic fluorophores using synthetically modified MS2 viral capsids. *J Am Chem Soc* 2013;**135**(8):3011–6.
22. Tong GJ, Hsiao SC, Carrico ZM, Francis MB. Viral capsid DNA aptamer conjugates as multivalent cell-targeting vehicles. *J Am Chem Soc* 2009;**131**(31):11174–8.
23. Obermeyer AC, Capehart SL, Jarman JB, Francis MB. Multivalent viral capsids with internal cargo for fibrin imaging. *PLoS One* 2014;**9**(6):e100678.
24. Carrico ZM, Romanini DW, Mehl RA, Francis MB. Oxidative coupling of peptides to a virus capsid containing unnatural amino acids. *Chem Commun* 2008;(10):1205–7.
25. Farkas ME, Aanei IL, Behrens CR, Tong GJ, Murphy ST, O'Neil JP, Francis MB. PET Imaging and biodistribution of chemically modified bacteriophage MS2. *Mol Pharm* 2013;**10**(1):69–76.
26. Stephanopoulos N, Carrico ZM, Francis MB. Nanoscale integration of sensitizing chromophores and porphyrins with bacteriophage MS2. *Angew Chem Int Ed Engl* 2009;**48**(50):9498–502.
27. El Muslemany KM, Twite AA, ElSohly AM, Obermeyer AC, Mathies RA, Francis MB. Photoactivated bioconjugation between ortho-azidophenols and anilines: a facile approach to biomolecular photopatterning. *J Am Chem Soc* 2014;**136**(36):12600–6.
28. Garimella PD, Datta A, Romanini DW, Raymond KN, Francis MB. Multivalent, high-relaxivity MRI contrast agents using rigid cysteine-reactive gadolinium complexes. *J Am Chem Soc* 2011;**133**(37):14704–9.
29. Wu W, Hsiao SC, Carrico ZM, Francis MB. Genome-free viral capsids as multivalent carriers for taxol delivery. *Angew Chem* 2009;**48**(50):9493–7.
30. Schlick TL, Ding Z, Kovacs EW, Francis MB. Dual-surface modification of the tobacco mosaic virus. *J Am Chem Soc* 2005;**127**(11):3718–23.
31. Wu M, Shi J, Fan D, Zhou Q, Wang F, Niu Z, Huang Y. Bio-behavior in normal and tumor-bearing mice of tobacco mosaic virus. *Biomacromolecules* 2013;**14**(11):4032–7.
32. Bruckman MA, Jiang K, Simpson EJ, Randolph LN, Luyt LG, Yu X, Steinmetz NF. Dual-modal magnetic resonance and fluorescence imaging of atherosclerotic plaques in vivo using VCAM-1 targeted tobacco mosaic virus. *Nano Lett* 2014;**14**(3):1551–8.
33. Bruckman MA, Hern S, Jiang K, Flask CA, Yu X, Steinmetz NF. Tobacco mosaic virus rods and spheres as supramolecular high-relaxivity MRI contrast agents. *J Mater Chem B* 2013;**1**(10):1482–90.
34. Yin Z, Nguyen HG, Chowdhury S, Bentley P, Bruckman MA, Miermont A, Gildersleeve JC, Wang Q, Huang X. Tobacco mosaic virus as a new carrier for tumor associated carbohydrate antigens. *Bioconjug Chem* 2012;**23**(8):1694–703.
35. Hu J, Wang P, Zhao X, Lv L, Yang S, Song B, Wang Q. Charge-transfer interactions for the fabrication of multifunctional viral nanoparticles. *Chem Commun* 2014;**50**(91):14125–8.
36. Sitasuwan P, Lee LA, Li K, Nguyen HG, Wang Q. RGD-conjugated rod-like viral nanoparticles on 2D scaffold improve bone differentiation of mesenchymal stem cells. *Front Chem* 2014;**2**: 31–31.
37. Chen L, Zhao X, Lin Y, Huang Y, Wang Q. A supramolecular strategy to assemble multifunctional viral nanoparticles. *Chem Commun* 2013;**49**(83):9678–80.
38. Bruckman MA, Liu J, Koley G, Li Y, Benicewicz B, Niu Z, Wang Q. Tobacco mosaic virus based thin film sensor for detection of volatile organic compounds. *J Mater Chem* 2010;**20**(27):5715–9.
39. Miller RA, Presley AD, Francis MB. Self-assembling light-harvesting systems from synthetically modified tobacco mosaic virus coat proteins. *J Am Chem Soc* 2007;**129**(11):3104–9.

40. Miller RA, Stephanopoulos N, McFarland JM, Rosko AS, Geissler PL, Francis MB. Impact of assembly state on the defect tolerance of TMV-based light harvesting arrays. *J Am Chem Soc* 2010;**132**(17):6068–74.
41. Obermeyer AC, Jarman JB, Francis MB. N-terminal modification of proteins with o-aminophenols. *J Am Chem Soc* 2014;**136**(27):9572–9.
42. Yin Z, Comellas-Aragones M, Chowdhury S, Bentley P, Kaczanowska K, BenMohamed L, Gildersleeve JC, Finn MG, Huang X. Boosting immunity to small tumor-associated carbohydrates with bacteriophage Q β capsids. *ACS Chem Biol* 2013;**8**(6):1253–62.
43. Hong V, Presolski SI, Ma C, Finn MG. Analysis and optimization of copper-catalyzed azide–alkyne cycloaddition for bioconjugation. *Angew Chem Int Ed* 2009;**48**(52):9879–83.
44. Mead G, Hiley M, Ng T, Fihn C, Hong K, Groner M, Miner W, Drugan D, Hollingsworth W, Udit AK. Directed polyvalent display of sulfated ligands on virus nanoparticles elicits heparin-like anticoagulant activity. *Bioconjug Chem* 2014;**25**(8):1444–52.
45. Pokorski JK, Hovlid ML, Finn MG. Cell targeting with hybrid Q β virus-like particles displaying epidermal growth factor. *Chem-biochem* 2011;**12**(16):2441–7.
46. Banerjee D, Liu AP, Voss NR, Schmid SL, Finn MG. Multivalent display and receptor-mediated endocytosis of transferrin on virus-like particles. *ChemBiochem* 2010;**11**(9):1273–9.
47. Manzenrieder F, Luxenhofer R, Retzlaff M, Jordan R, Finn MG. Stabilization of virus-like particles with poly(2-oxazoline)s. *Angew Chem* 2011;**50**(11):2601–5.
48. Steinmetz NF, Hong V, Spoerke ED, Lu P, Breitenkamp K, Finn MG, Manchester M. Buckyballs meet viral nanoparticles: candidates for biomedicine. *J Am Chem Soc* 2009;**131**(47):17093–5.
49. Astronomo RD, Kaltgrad E, Udit AK, Wang SK, Doores KJ, Huang CY, Pantophlet R, Paulson JC, Wong CH, Finn MG, Burton DR. Defining criteria for oligomannose immunogens for HIV using icosahedral virus capsid scaffolds. *Chem Biol* 2010;**17**(4):357–70.
50. Kaltgrad E, O'Reilly MK, Liao L, Han S, Paulson JC, Finn MG. On-virus construction of polyvalent glycan ligands for cell-surface receptors. *J Am Chem Soc* 2008;**130**(14):4578–9.
51. Prasuhn JDE, Yeh RM, Obenaus A, Manchester M, Finn MG. Viral MRI contrast agents: coordination of Gd by native virions and attachment of Gd complexes by azide–alkyne cycloaddition. *Chem Commun* 2007;(12):1269–71.
52. Hovlid ML, Lau JL, Breitenkamp K, Higginson CJ, Laufer B, Manchester M, Finn MG. Encapsidated atom-transfer radical polymerization in Q β virus-like nanoparticles. *ACS Nano* 2014;**8**(8):8003–14.
53. Qazi S, Uchida M, Usselman R, Shearer R, Edwards E, Douglas T. Manganese(III) porphyrins complexed with P22 virus-like particles as T1-enhanced contrast agents for magnetic resonance imaging. *J Biol Inorg Chem* 2014;**19**(2):237–46.
54. Lucon J, Edwards E, Qazi S, Uchida M, Douglas T. Atom transfer radical polymerization on the interior of the P22 capsid and incorporation of photocatalytic monomer crosslinks. *Eur Polym J* 2013;**49**(10):2976–85.
55. Min J, Moon H, Yang HJ, Shin H-H, Hong SY, Kang S. Development of P22 viral capsid nanocomposites as anti-cancer drug, bortezomib (BTZ), delivery nanoplatfoms. *Macromol Biosci* 2014;**14**(4):557–64.
56. Qazi S, Liepold LO, Abedin MJ, Johnson B, Prevelige P, Frank JA, Douglas T. P22 viral capsids as nanocomposite high-relaxivity MRI contrast agents. *Mol Pharm* 2013;**10**(1):11–7.
57. Kang S, Lander GC, Johnson JE, Prevelige PE. Development of bacteriophage P22 as a platform for molecular display: genetic and chemical modifications of the procapsid exterior surface. *Chem-biochem* 2008;**9**(4):514–8.
58. Anand P, O'Neil A, Lin E, Douglas T, Holford M. Tailored delivery of analgesic ziconotide across a blood brain barrier model using viral nanocontainers. *Sci Rep* 2015;**5**:12497.
59. Servid A, Jordan P, O'Neil A, Prevelige P, Douglas T. Location of the bacteriophage P22 coat protein C-terminus provides opportunities for the design of capsid-based materials. *Biomacromolecules* 2013;**14**(9):2989–95.
60. Brunel FM, Lewis JD, Destito G, Steinmetz NF, Manchester M, Stuhlmann H, Dawson PE. Hydrazone ligation strategy to assemble multifunctional viral nanoparticles for cell imaging and tumor targeting. *Nano Lett* 2010;**10**(3):1093–7.
61. Hovlid ML, Steinmetz NF, Laufer B, Lau JL, Kuzelka J, Wang Q, Hyypä T, Nemerow GR, Kessler H, Manchester M, Finn MG. Guiding plant virus particles to integrin-displaying cells. *Nanoscale* 2012;**4**(12):3698–705.
62. Destito G, Yeh R, Rae CS, Finn MG, Manchester M. Folic acid-mediated targeting of cowpea mosaic virus particles to tumor cells. *Chem Bio* 2007;**14**(10):1152–62.
63. Sen Gupta S, Kuzelka J, Singh P, Lewis WG, Manchester M, Finn MG. Accelerated bioorthogonal conjugation: a practical method for the ligation of diverse functional molecules to a polyvalent virus scaffold. *Bioconjug Chem* 2005;**16**(6):1572–9.
64. Comellas-Aragones M, de la Escosura A, Dirks AJ, van der Ham A, Fusté-Cuñé A, Cornelissen JJLM, Nolte RJM. Controlled integration of polymers into viral capsids. *Biomacromolecules* 2009;**10**(11):3141–7.
65. Singh P, Prasuhn D, Yeh RM, Destito G, Rae CS, Osborn K, Finn MG, Manchester M. Bio-distribution, toxicity and pathology of cowpea mosaic virus nanoparticles in vivo. *J Control Release* 2007;**120**(1–2):41–50.
66. Steinmetz NF, Manchester M. PEGylated viral nanoparticles for biomedicine: the impact of PEG chain length on VNP cell interactions in vitro and ex vivo. *Biomacromolecules* 2009;**10**(4):784–92.
67. Shukla S, Ablack AL, Wen AM, Lee KL, Lewis JD, Steinmetz NF. Increased tumor homing and tissue penetration of the filamentous plant viral nanoparticle Potato virus X. *Mol Pharm* 2013;**10**(1):33–42.
68. Steinmetz NF, Lomonosoff GP, Evans DJ. Decoration of cowpea mosaic virus with multiple, redox-active, organometallic complexes. *Small* 2006;**2**(4):530–3.
69. Wu Z, Chen K, Yildiz I, Dirksen A, Fischer R, Dawson PE, Steinmetz NF. Development of viral nanoparticles for efficient intracellular delivery. *Nanoscale* 2012;**4**(11):3567–76.
70. Chatterji A, Ochoa W, Shamieh L, Salakian SP, Wong SM, Clinton G, Ghosh P, Lin T, Johnson JE. Chemical conjugation of heterologous proteins on the surface of Cowpea mosaic virus. *Bioconjug Chem* 2004;**15**(4):807–13.

71. Noad R, Roy P. Virus-like particles as immunogens. *Trends Microbiol* 2003;**11**(9):438–44.
72. Akahata W, Yang Z-Y, Andersen H, Sun S, Holdaway HA, Kong W-P, Lewis MG, Higgs S, Rossmann MG, Rao S, Nabel GJ. A virus-like particle vaccine for epidemic Chikungunya virus protects nonhuman primates against infection. *Nat Med* 2010;**16**(3):334–8.
73. Naskalska A, Pyrc K. Virus like particles as immunogens and universal nanocarriers. *Pol J Microbiol* 2015;**64**(1):3–13.
74. Roldao A, Mellado MC, Castilho LR, Carrondo MJ, Alves PM. Virus-like particles in vaccine development. *Expert Rev Vaccines* 2010;**9**(10):1149–76.
75. Kushnir N, Streatfield SJ, Yusibov V. Virus-like particles as a highly efficient vaccine platform: diversity of targets and production systems and advances in clinical development. *Vaccine* 2012;**31**(1):58–83.
76. Dharmarwardana M, Martins AF, Chen Z, Palacios PM, Nowak CM, Welch RP, Li S, Luzuriaga MA, Bleris L, Pierce BS, Sherry AD, Gassensmith JJ. Nitroxyl modified tobacco mosaic virus as a metal-free high-relaxivity MRI and EPR active superoxide sensor. *Mol Pharm* 2018;**15**(8):2973–83.
77. Nanduri V, Balasubramanian S, Sista S, Vodyanoy VJ, Simonian AL. Highly sensitive phage-based biosensor for the detection of β -galactosidase. *Anal Chim Acta* 2007;**589**(2):166–72.
78. Moon J-S, Park M, Kim W-G, Kim C, Hwang J, Seol D, Kim C-S, Sohn J-R, Chung H, Oh J-W. M-13 bacteriophage based structural color sensor for detecting antibiotics. *Sens Actuators B Chem* 2017;**240**:757–62.
79. Molino NM, Wang S-W. Caged protein nanoparticles for drug delivery. *Curr Opin Biotechnol* 2014;**28**:75–82.
80. Schwarz B, Douglas T. Development of virus-like particles for diagnostic and prophylactic biomedical applications. *Wiley Interdiscip Rev Nanomed Nanobiotechnol* 2015;**7**(5):722–35.
81. Lee KL, Shukla S, Wu M, Ayat NR, El Sanadi CE, Wen AM, Edelbrock JF, Pokorski JK, Commandeur U, Dubyak GR, Steinmetz NF. Stealth filaments: polymer chain length and conformation affect the in vivo fate of PEGylated potato virus X. *Acta Biomaterialia* 2015;**19**:166–79.
82. Aanei IL, ElSohly AM, Farkas ME, Netirojjanakul C, Regan M, Taylor Murphy S, O'Neil JP, Seo Y, Francis MB. Biodistribution of antibody-MS2 viral capsid conjugates in breast cancer models. *Mol Pharm* 2016;**13**(11):3764–72.
83. Prasuhn Jr DE, Singh P, Strable E, Brown S, Manchester M, Finn MG. Plasma clearance of bacteriophage Qbeta particles as a function of surface charge. *J Am Chem Soc* 2008;**130**(4):1328–34.
84. Agrawal A, Manchester M. Differential uptake of chemically modified cowpea mosaic virus nanoparticles in macrophage subpopulations present in inflammatory and tumor microenvironments. *Biomacromolecules* 2012;**13**(10):3320–6.
85. Lee H, Benjamin CE, Nowak CM, Tuong LH, Welch RP, Chen Z, Dharmarwardana M, Murray KW, Bleris L, D'Arcy S, Gassensmith JJ. Regulating the uptake of viral nanoparticles in macrophage and cancer cells via a pH switch. *Mol Pharm* 2018;**15**(8):2984–90.
86. Mishra P, Nayak B, Dey RK. PEGylation in anti-cancer therapy: an overview. *Asian J Pharm Sci* 2016;**11**(3):337–48.
87. Cho J, Lim SI, Yang BS, Hahn YS, Kwon I. Generation of therapeutic protein variants with the human serum albumin binding capacity via site-specific fatty acid conjugation. *Sci Rep* 2017;**7**(1):18041.
88. Gulati NM, Pitek AS, Czapar AE, Stewart PL, Steinmetz NF. The in vivo fates of plant viral nanoparticles camouflaged using self-proteins: overcoming immune recognition. *J Mater Chem B* 2018;**6**(15):2204–16.
89. Minko T, Dharap SS, Pakunlu RI, Wang Y. Molecular targeting of drug delivery systems to cancer. *Curr Drug Targets* 2004;**5**(4):389–406.
90. Rohovie MJ, Nagasawa M, Swartz JR. Virus-like particles: next-generation nanoparticles for targeted therapeutic delivery. *Bioeng Transl Med* 2017;**2**(1):43–57.
91. Chen Z, Li N, Chen L, Lee J, Gassensmith JJ. Dual functionalized bacteriophage Qbeta as a photocaged drug carrier. *Small* 2016;**12**(33):4563–71.
92. Pokorski JK, Steinmetz NF. The art of engineering viral nanoparticles. *Mol Pharm* 2011;**8**(1):29–43.
93. Kundig TM, Klimek L, Schendzielorz P, Renner WA, Senti G, Bachmann MF. Is the allergen really needed in allergy immunotherapy? *Current Treat Options Allergy* 2015;**2**(1):72–82.
94. Engeroff P, Caviezel F, Stormi F, Thoms F, Vogel M, Bachmann MF. Allergens displayed on virus-like particles are highly immunogenic but fail to activate human mast cells. *Allergy* 2018;**73**(2):341–9.
95. Grgacic EV, Anderson DA. Virus-like particles: passport to immune recognition. *Methods* 2006;**40**(1):60–5.
96. Chen Z, Detvo ST, Pham E, Gassensmith JJ. Making conjugation-induced fluorescent PEGylated virus-like particles by dibromomaleimide-disulfide chemistry. *J Vis Exp* 2018;**135**:e57712.
97. van Zyl AR, Hitzeroth II. Purification of virus-like particles (VLPs) from plants. *Methods Mol Biol* 2016;**1404**:569–79.
98. Zeltins A. Construction and characterization of virus-like particles: a review. *Mol Biotechnol* 2013;**53**(1):92–107.
99. Fuenmayor J, Gòdia F, Cervera L. Production of virus-like particles for vaccines. *New Biotechnol* 2017;**39**:174–80.
100. Chen Z, Li N, Li S, Dharmarwardana M, Schlimme A, Gassensmith JJ. Viral chemistry: the chemical functionalization of viral architectures to create new technology. *Wiley Interdiscip Rev Nanomed Nanobiotechnol* 2016;**8**(4):512–34.
101. Li K, Nguyen HG, Lu X, Wang Q. Viruses and their potential in bioimaging and biosensing applications. *Analyst* 2010;**135**(1):21–7.
102. Tagit O, de Ruiter MV, Brasch M, Ma Y, Cornelissen JLM. Quantum dot encapsulation in virus-like particles with tuneable structural properties and low toxicity. *RSC Adv* 2017;**7**(60):38110–8.
103. Yildiz I, Shukla S, Steinmetz NF. Applications of viral nanoparticles in medicine. *Curr Opin Biotechnol* 2011;**22**(6):901–8.
104. Robertson KL, Liu JL. Engineered viral nanoparticles for flow cytometry and fluorescence microscopy applications. *Wiley Interdiscip Rev Nanomed Nanobiotechnol* 2012;**4**(5):511–24.
105. Chen Z, Boyd SD, Calvo JS, Murray KW, Mejia GL, Benjamin CE, Welch RP, Winkler DD, Meloni G, D'Arcy S, Gassensmith JJ. Fluorescent functionalization across quaternary structure in a virus-like particle. *Bioconjug Chem* 2017;**28**(9):2277–83.
106. Lewis JD, Destito G, Zijlstra A, Gonzalez MJ, Quigley JP, Manchester M, Stuhlmann H. Viral nanoparticles as tools for intravital vascular imaging. *Nat Med* 2006;**12**(3):354–60.

107. Steinmetz NF, Ablack AL, Hickey JL, Ablack J, Manocha B, Mymryk JS, Luyt LG, Lewis JD. Intravital imaging of human prostate cancer using viral nanoparticles targeted to gastrin-releasing peptide receptors. *Small* 2011;**7**(12):1664–72.
108. Carrico ZM, Farkas ME, Zhou Y, Hsiao SC, Marks JD, Chokhwalwa H, Clark DS, Francis MB. N-Terminal labeling of filamentous phage to create cancer marker imaging agents. *ACS Nano* 2012;**6**(8):6675–80.
109. Wen AM, Rambhia PH, French RH, Steinmetz NF. Design rules for nanomedical engineering: from physical virology to the applications of virus-based materials in medicine. *J Biol Phys* 2013;**39**(2):301–25.
110. Bruckman MA, Randolph LN, VanMeter A, Hern S, Shoffstall AJ, Taurog RE, Steinmetz NF. Biodistribution, pharmacokinetics, and blood compatibility of native and PEGylated tobacco mosaic virus nano-rods and -spheres in mice. *Virology* 2014;**449**:163–73.
111. Liepold L, Anderson S, Willits D, Oltrogge L, Frank JA, Douglas T, Young M. Viral capsids as MRI contrast agents. *Magn Reson Med* 2007;**58**(5):871–9.
112. Sowers MA, McCombs JR, Wang Y, Paletta JT, Morton SW, Dreaden EC, Boska MD, Ottaviani MF, Hammond PT, Rajca A, Johnson JA. Redox-responsive branched-bottlebrush polymers for in vivo MRI and fluorescence imaging. *Nat Commun* 2014;**5**: 5460–5460.
113. Merbach, A.; Helm, L.; Tóth, É., 2013; p 0.
114. Nguyen HVT, Chen Q, Paletta JT, Harvey P, Jiang Y, Zhang H, Boska MD, Ottaviani MF, Jasanoff A, Rajca A, Johnson JA. Nitroxide-based macromolecular contrast agents with unprecedented transverse relaxivity and stability for magnetic resonance imaging of tumors. *ACS Central Science* 2017;**3**(7):800–11.
115. Meldrum T, Seim KL, Bajaj VS, Palaniappan KK, Wu W, Francis MB, Wemmer DE, Pines A. A xenon-based molecular sensor assembled on an MS2 viral capsid scaffold. *J Am Chem Soc* 2010;**132**(17):5936–7.
116. Xiao L, Zhu A, Xu Q, Chen Y, Xu J, Weng J. Colorimetric biosensor for detection of cancer biomarker by Au nanoparticle-decorated Bi₂Se₃ nanosheets. *ACS Appl Mater Interfaces* 2017;**9**(8):6931–40.
117. Wang P, Xu G, Qin L, Li Y, Li R. Cell-based biosensors and its application in biomedicine. *Sens Actuators B Chem* 2005;**108**(1–2): 576–84.
118. Kara P, de la Escosura-Muniz A, Maltez-da Costa M, Guix M, Ozsoz M, Merkoci A. Aptamers based electrochemical biosensor for protein detection using carbon nanotubes platforms. *Biosens Bioelectron* 2010;**26**(4):1715–8.
119. Yoo EH, Lee SY. Glucose biosensors: an overview of use in clinical practice. *Sensors* 2010;**10**(5):4558–76.
120. Mao C, Liu A, Cao B. Virus-based chemical and biological sensing. *Angew Chem* 2009;**48**(37):6790–810.
121. Tscherne DM, Manicassamy B, Garcia-Sastre A. An enzymatic virus-like particle assay for sensitive detection of virus entry. *J Virol Methods* 2010;**163**(2):336–43.
122. Koch C, Wabbel K, Eber FJ, Krolla-Sidenstein P, Azucena C, Gliemann H, Eiben S, Geiger F, Wege C. Modified TMV particles as beneficial scaffolds to present sensor enzymes. *Front Plant Sci* 2015;**6**(1137).
123. Jablonski M, Koch C, Bronder TS, Poghossian A, Wege C, Schöning MJ. Field-effect biosensors modified with tobacco mosaic virus nanotubes as enzyme nanocarrier. *Proceedings* 2017;**1**(4).
124. Poghossian A, Jablonski M, Koch C, Bronder TS, Rolka D, Wege C, Schöning MJ. Field-effect biosensor using virus particles as scaffolds for enzyme immobilization. *Biosens Bioelectron* 2018;**110**:168–74.
125. Bäcker M, Koch C, Eiben S, Geiger F, Eber F, Gliemann H, Poghossian A, Wege C, Schöning MJ. Tobacco mosaic virus as enzyme nanocarrier for electrochemical biosensors. *Sens Actuators B Chem* 2017;**238**:716–22.
126. Kim D, Daniel WL, Mirkin CA. Microarray-based multiplexed scanometric immunoassay for protein cancer markers using gold nanoparticle probes. *Anal Chem* 2009;**81**(21):9183–7.
127. Brasino M, Lee JH, Cha JN. Creating highly amplified enzyme-linked immunosorbent assay signals from genetically engineered bacteriophage. *Anal Biochem* 2015;**470**:7–13.
128. Lee JH, Cha JN. Amplified protein detection through visible plasmon shifts in gold nanocrystal solutions from bacteriophage platforms. *Anal Chem* 2011;**83**(9):3516–9.
129. Lee JH, Xu PF, Domaille DW, Choi C, Jin S, Cha JN. M13 bacteriophage as materials for amplified surface enhanced Raman scattering protein sensing. *Adv Funct Mater* 2013;**24**(14):2079–84.
130. Domaille DW, Lee JH, Cha JN. High density DNA loading on the M13 bacteriophage provides access to colorimetric and fluorescent protein microarray biosensors. *Chem Commun (Camb)* 2013;**49**(17):1759–61.
131. Guo J, Zhao X, Hu J, Lin Y, Wang Q. Tobacco mosaic virus with peroxidase-like activity for cancer cell detection through colorimetric assay. *Mol Pharm* 2018;**15**(8):2946–53.
132. Ben-Yoav H, Brown A, Pomerantseva E, L Kelly D, N Culver J, Ghodssi R. Tobacco mosaic virus biotemplated electrochemical biosensor. 2012.
133. Zang F, Gerasopoulos K, Brown AD, Culver JN, Ghodssi R. Capillary microfluidics-assembled virus-like particle bio-nanoreceptor interfaces for label-free biosensing. *ACS Appl Mater Interfaces* 2017;**9**(10):8471–9.
134. Jia Y, Qin M, Zhang H, Niu W, Li X, Wang L, Li X, Bai Y, Cao Y, Feng X. Label-free biosensor: a novel phage-modified Light Addressable Potentiometric Sensor system for cancer cell monitoring. *Biosens Bioelectron* 2007;**22**(12):3261–6.
135. Brun MJ, Gomez EJ, Suh J. Stimulus-responsive viral vectors for controlled delivery of therapeutics. *J Control Release* 2017;**267**:80–9.
136. Hubbell JA, Chilkoti A. Nanomaterials for drug delivery. *Science* 2012;**337**(6092):303–5.
137. Suri SS, Fenniri H, Singh B. Nanotechnology-based drug delivery systems. *J Occup Med Toxicol* 2007;**2**:16.
138. Li SD, Huang L. Pharmacokinetics and biodistribution of nanoparticles. *Mol Pharm* 2008;**5**(4):496–504.
139. Ventola CL. Progress in nanomedicine: approved and investigational nanodrugs. *PT* 2017;**42**(12):742–55.
140. Moghimi SM, Szebeni J. Stealth liposomes and long circulating nanoparticles: critical issues in pharmacokinetics, opsonization and protein-binding properties. *Prog Lipid Res* 2003;**42**(6):463–78.
141. Ishida T, Masuda K, Ichikawa T, Ichihara M, Irimura K, Kiwada H. Accelerated clearance of a second injection of PEGylated liposomes in mice. *Int J Pharm* 2003;**255**(1):167–74.

142. Ishida T, Ichihara M, Wang X, Kiwada H. Spleen plays an important role in the induction of accelerated blood clearance of PEGylated liposomes. *J Control Release* 2006;**115**(3):243–50.
143. Ishida T, Harada M, Wang XY, Ichihara M, Irimura K, Kiwada H. Accelerated blood clearance of PEGylated liposomes following preceding liposome injection: effects of lipid dose and PEG surface-density and chain length of the first-dose liposomes. *J Control Release* 2005;**105**(3):305–17.
144. Gabizon A, Tzemach D, Mak L, Bronstein M, Horowitz AT. Dose dependency of pharmacokinetics and therapeutic efficacy of pegylated liposomal doxorubicin (DOXIL) in murine models. *J Drug Target* 2002;**10**(7):539–48.
145. Allen TM, Cullis PR. Liposomal drug delivery systems: from concept to clinical applications. *Adv Drug Deliv Rev* 2013;**65**(1):36–48.
146. Sercombe L, Veerati T, Moheimani F, Wu SY, Sood AK, Hua S. Advances and challenges of liposome assisted drug delivery. *Front Pharmacol* 2015;**6**: 286-286.
147. Pan Y, Zhang Y, Jia T, Zhang K, Li J, Wang L. Development of a microRNA delivery system based on bacteriophage MS2 virus-like particles. *FEBS J* 2012;**279**(7):1198–208.
148. Prel A, Caval V, Gayon R, Ravassard P, Duthoit C, Payen E, Maouche-Chretien L, Creneguy A, Nguyen TH, Martin N, Piver E, Sevrain R, Lamouroux L, Leboulch P, Deschaseaux F, Bouille P, Sensebe L, Pages JC. Highly efficient in vitro and in vivo delivery of functional RNAs using new versatile MS2-chimeric retrovirus-like particles. *Mol Ther Methods Clin Dev* 2015;**2** (2329-0501 (Print)).
149. Lam P, Steinmetz NF. Plant viral and bacteriophage delivery of nucleic acid therapeutics. *Wiley Interdiscip Rev Nanomed Nanobiotechnol* 2018;**10**(1):e1487.
150. Yao Y, Jia T, Pan Y, Gou H, Li Y, Sun Y, Zhang R, Zhang K, Lin G, Xie J, Li J, Wang L. Using a novel microRNA delivery system to inhibit osteoclastogenesis. *Int J Mol Sci* 2015;**16**(4):8337–50.
151. Kwak M, Minten IJ, Anaya D-M, Musser AJ, Brasch M, Nolte RJM, Müllen K, Cornelissen JJLM, Herrmann A. Virus-like particles templated by DNA micelles: a general method for loading virus nanocarriers. *J Am Chem Soc* 2010;**132**(23):7834–5.
152. Touze A, Coursaget P. In vitro gene transfer using human papillomavirus-like particles. *Nucleic Acids Res* 1998;**26**(5):1317–23.
153. Xu, Y. F.; Zhang YQ - Xu, X. M.; Xu Xm Fau - Song, G. X.; Song, G. X., Papillomavirus virus-like particles as vehicles for the delivery of epitopes or genes. *Arch Virol* (0304-8608 [Print]).
154. Lau JL, Baksh MM, Fiedler JD, Brown SD, Kussrow A, Bornhop DJ, Ordoukhanian P, Finn MG. Evolution and protein packaging of small-molecule RNA aptamers. *ACS Nano* 2011;**5**(10):7722–9.
155. Fiedler JD, Brown SD, Lau JL, Finn MG. RNA-directed packaging of enzymes within virus-like particles. *Angew Chem* 2010;**49**(50):9648–51.
156. Benjamin CE, Chen Z, Kang P, Wilson BA, Li N, Nielsen SO, Qin Z, Gassensmith JJ. Site-selective nucleation and size control of gold nanoparticle photothermal antennae on the pore structures of a virus. *J Am Chem Soc* 2018;**140**(49):17226–33.
157. Franke CE, Czapar AE, Patel RB, Steinmetz NF. Tobacco mosaic virus-delivered cisplatin restores efficacy in platinum-resistant ovarian cancer cells. *Mol Pharm* 2018;**15**(8):2922–31.
158. Zeng Q, Wen H, Wen Q, Chen X, Wang Y, Xuan W, Liang J, Wan S. Cucumber mosaic virus as drug delivery vehicle for doxorubicin. *Biomaterials* 2013;**34**(19):4632–42.
159. Pitek AS, Wang Y, Gulati S, Gao H, Stewart PL, Simon DI, Steinmetz NF. Elongated plant virus-based nanoparticles for enhanced delivery of thrombolytic therapies. *Mol Pharm* 2017;**14**(11):3815–23.
160. Aljabali AA, Shukla S, Lomonosoff GP, Steinmetz NF, Evans DJ. CPMV-DOX delivers. *Mol Pharm* 2013;**10**(1):3–10.
161. Vernekar AA, Berger G, Czapar AE, Veliz FA, Wang DI, Steinmetz NF, Lippard SJ. Speciation of phenanthriplatin and its analogs in the core of tobacco mosaic virus. *J Am Chem Soc* 2018;**140**(12):4279–87.
162. Masarapu H, Patel BK, Chariou PL, Hu H, Gulati NM, Carpenter BL, Ghiladi RA, Shukla S, Steinmetz NF. Physalis mottle virus-like particles as nanocarriers for imaging reagents and drugs. *Biomacromolecules* 2017;**18**(12):4141–53.
163. Kaczmarczyk SJ, Sitaraman K, Young HA, Hughes SH, Chatterjee DK. Protein delivery using engineered virus-like particles. *Proc Natl Acad Sci USA* 2011;**108**(41):16998–7003.
164. Minten IJ, Hendriks LJA, Nolte RJM, Cornelissen JJLM. Controlled encapsulation of multiple proteins in virus capsids. *J Am Chem Soc* 2009;**131**(49):17771–3.
165. Setaro F, Brasch M, Hahn U, Koay MST, Cornelissen JJLM, de la Escosura A, Torres T. Generation-dependent templated self-assembly of biohybrid protein nanoparticles around photosensitizer dendrimers. *Nano Lett* 2015;**15**(2):1245–51.
166. Madaan K, Kumar S, Poonia N, Lather V, Pandita D. Dendrimers in drug delivery and targeting: drug-dendrimer interactions and toxicity issues. *J Pharm BioAllied Sci* 2014;**6**(3):139–50.
167. Miao Y, Johnson JE, Ortoleva PJ. All-atom multiscale simulation of cowpea chlorotic mottle virus capsid swelling. *J Phys Chem B* 2010;**114**(34):11181–95.
168. Wilts BD, Schaap IAT, Schmidt CF. Swelling and softening of the cowpea chlorotic mottle virus in response to pH shifts. *Biophys J* 2015;**108**(10):2541–9.
169. Asensio MA, Morella NM, Jakobson CM, Hartman EC, Glasgow JE, Sankaran B, Zwart PH, Tullman-Ercek D. A selection for assembly reveals that a single amino acid mutant of the bacteriophage MS2 coat protein forms a smaller virus-like particle. *Nano Lett* 2016;**16**(9):5944–50.
170. Cadena-Nava RD, Comas-Garcia M, Garmann RF, Rao AL, Knobler CM, Gelbart WM. Self-assembly of viral capsid protein and RNA molecules of different sizes: requirement for a specific high protein/RNA mass ratio. *J Virol* 2012;**86**(6):3318–26.
171. Rurup WF, Verbij F, Koay MST, Blum C, Subramaniam V, Cornelissen JJLM. Predicting the loading of virus-like particles with fluorescent proteins. *Biomacromolecules* 2014;**15**(2):558–63.
172. Stephanopoulos N, Tong GJ, Hsiao SC, Francis MB. Dual-surface modified virus capsids for targeted delivery of photodynamic agents to cancer cells. *ACS Nano* 2010;**4**(10):6014–20.
173. Zhang X, Xin L, Li S, Fang M, Zhang J, Xia N, Zhao Q. Lessons learned from successful human vaccines: delineating key epitopes by dissecting the capsid proteins. *Hum Vaccines Immunother* 2015;**11**(5):1277–92.
174. Jegerlehner A, Zabel F, Langer A, Dietmeier K, Jennings GT, Saudan P, Bachmann MF. Bacterially produced recombinant influenza vaccines based on virus-like particles. *PLoS One* 2013;**8**(11):e78947.

175. Storni T, Ruedl C, Schwarz K, Schwendener RA, Renner WA, Bachmann MF. Nonmethylated CG motifs packaged into virus-like particles induce protective cytotoxic T cell responses in the absence of systemic side effects. *J Immunol* 2004;**172**(3):1777–85.
176. Cornuz J, Zwahlen S, Jungi WF, Osterwalder J, Klingler K, van Melle G, Bangala Y, Guessous I, Müller P, Willers J, Maurer P, Bachmann MF, Cerny T. A vaccine against nicotine for smoking cessation: a randomized controlled trial. *PLoS One* 2008;**3**(6):e2547.
177. Watanabe T, Watanabe S, Neumann G, Kida H, Kawaoka Y. Immunogenicity and protective efficacy of replication-incompetent influenza virus-like particles. *J Virol* 2002;**76**(2):767.
178. Li B, Yuan Z, Hung H-C, Ma J, Jain P, Tsao C, Xie J, Zhang P, Lin X, Wu K, Jiang S. Revealing the immunogenic risk of polymers. *Angew Chem Int Ed* 2018;**57**(42):13873–6.